Deliverable 4-A & B: Report & Demonstration of Performance rating of geotechnical assets using remotely measured displacement

Rudiger Escobar Wolf, El Hachemi Bouali, Samantha Justice, Daniel Cerminaro, Thomas Oommen, and Stanley J. Vitton

Michigan Technological University

USDOT Cooperative Agreement No. **RITARS-14-H-MTU**

Due on: December 31, 2015

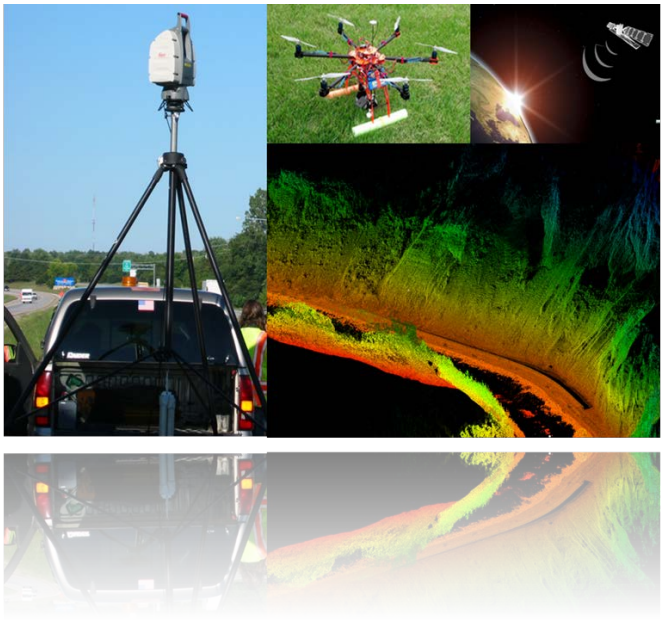

Principal Investigator: **Dr. Thomas Oommen, Associate Professor**
Department of Geological and Mining Engineering and Sciences
Michigan Technological University
1400 Townsend Drive
Houghton, MI 49931
(906) 487-2045
toommen@mtu.edu
Program Manager: **Caesar Singh, P.E.**
Director, University Grants Program/Program Manager
OST-Office of the Assistant Secretary for Research and Technology
U.S. Dept. of Transportation
1200 New Jersey Avenue, SE, E35-336
Washington, DC 20590
(202) 366-3252
Caesar.Singh@dot.gov

Michigan Tech

TABLE OF CONTENTS

Acknowledgements

This work is supported by the US Department of Transportation, through the Office of the Assistant Secretary for Research and Technology (USDOT OST-R). The views, opinions, findings, and conclusions reflected in this paper are the responsibility of the authors only and do not represent the official policy or position of the USDOT OST-R, or any state or other entity. Additional information regarding this project can be found at www.mtri.org/geoasset. We also acknowledge European Space Agency support to obtain all ERS-1, ERS-2, and ENVISAT SAR data.

GLOSSARY OF TERMS

ALOS	Advanced Land Observing Satellite
AASHTO	American Association of State Highway and Transportation Officials
COSMO-SkyMed	Constellation of small Satellites for the Mediterranean basin Observation
DEM	Digital Elevation Model
DSLR	Digital single-lens reflex
DSS	Decision Support System
ENVISAT	Environmental Satellite
ERS	European Remote Sensing Satellite
FAA	Federal Aviation Administration
GAM	Geotechnical Asset Management
GB	Giga-byte
GNSS	Global Navigation Satellite System
GPS	Global Positioning System
InSAR	Interferometric Synthetic Aperture Radar
LiDAR	Light Detection and Ranging
Meteor-3M	Russian polar orbiting satellites
PALSAR	Phased Array type L-band Synthetic Aperture Radar
RADARSAT-1 and 2	Radar Satellite 1 and 2
RAM	Random access memory
RMSE	Root mean squared error
RTK	Real-time kinematic
Sentinel-1A and 1B	European Space Agency radar imaging satellites
SEOSAR/Paz	Satélite Español de Observación SAR (Spanish SAR observation satellite)
SFM	Structure from Motion
TerraSAR-X	German radar earth observation satellite
UAV	Unmanned aerial vehicle
USDOT/OST-R	US Department of Transportation, through the Office of the Assistant Secretary for Research and Technology
USGS	Unites States Geological Survey
VTOL	Vertical takeoff and landing

EXECUTIVE SUMMARY: DELIVERABLE 4-A & B

Overall Goal of this Deliverable: The objective of this report is to evaluate and demonstrate how remotely measured displacement values can be used to rate the condition of geotechnical assets. In this study, we present a multi-tier approach in which different levels of analysis are followed, starting with a large-scale, low-resolution level in which the most critical areas are identified and flagged for further in-depth analysis, at the following levels of the process. At each level, the analysis output gives a diagnostic of the asset as either not needing immediate attention or in need of further actions. If further steps are needed, they are grouped into two categories: further analysis, if the current level is non-conclusive enough, or a set of explicit actions that have to be taken to avoid the asset deterioration and loss of performance.

The multi-tier approach is demonstrated using two case studies: a slope stability analysis along a rail corridor in Nevada and a retaining wall near Detroit. The specific case studies use InSAR, LiDAR, and Photogrammetric remote sensing techniques as applicable. A similar multi-tier approach can be adopted for other geotechnical assets.

1. Introduction

1.1. Geotechnical asset management: performance of assets and their monitoring

1.1.1. The asset management paradigm

The term *asset management* is defined differently by each individual, government agency, or corporation, yet essentially means the same thing. In general, any actions implemented to maintain, preserve, or to perpetuate an asset's optimal performance level throughout its lifespan fall under the asset management umbrella. Transportation agencies each have their own official term. In a report entitled *Strategy for improving asset management practices*, the Australian road transport and traffic agencies association (Austroads) defined asset management as "...a comprehensive and structured approach to the long-term management of assets as tools for the efficient and effective delivery of community benefits" (Austroads 1997). Two years later the Federal Highway Administration (FHWA) expanded on this definition:

> "[Asset management is] a systematic approach of maintaining, upgrading, and operating physical assets cost effectively. It combines engineering principles with sound business practices and economic theory, and it provides tools to facilitate a more organized, logical approach to decisionmaking. Thus, asset management provides a framework for handling both short- and long-range planning." (p8 FHWA 1999)

Iterations of the asset management definition have been produced since and include portions of the FHWA definition. For example, the Michigan Department of Transportation (MDOT) defines asset management as "...a process to strategically manage our transportation system in a cost-effective and efficient manner" (MDOT 2015); Flintsch & Bryant, Jr. (2006) define it as "...a strategic approach to the optimal allocation of resources for the management, operation, maintenance, and preservation of transportation infrastructure"; the National Cooperative Highway Research Program (NCHRP) describe a portion of it as "...a strategic and systematic process of operating, maintaining, upgrading, and expanding physical assets effectively throughout their life cycle…" (Cambridge Systematics, Inc., et al. 2002). Regardless of the myriad of definitions, an agreement on the basic asset management process requires maintenance, management, and preservation of all assets along the transportation corridor.

Although many goals of asset management are included in the definitions above, the American Association of State Highway and Transportation (AASHTO) summarized the goals into three general

statements (pS-1, Cambridge Systematics, Inc., et al. 2002). The first goal is to “build, preserve, and operate facilities” in a manner that is more “cost-effective” and with an improvement in “asset performance.” The second goal is focused towards the consumers and general public and that is to obtain the “best value for the public tax dollar spent.” The third goal, which is more political, is to “enhance the credibility and accountability of the transportation agency to its governing executive and legislative bodies.” Of these three goals, methodologies towards accomplishing the first two goals have been studied in great detail, as the third goal is a byproduct of the first two.

Current practices in asset management vary greatly by transportation agency and again by asset type. The initial asset management approach was to divide focus by asset type and then create individual asset management programs. This resulted in the generation of individual asset management programs for bridges, pavement, geotechnical assets, slopes, and embankments, to name a few. The obvious problem with this divide-and-conquer approach is that separate management plans do not share data or information with any other plan. This can pose a problem since a variety of assets share the same transportation corridor. For example, one slope failure could potentially affect assets categorized in all management programs listed above. Even worse, some types of asset management systems do not have standard procedures between state DOTs or transportation agencies; Vessely (2013) laments “...there does not appear to be a standard practice for geotechnical asset management within state and federal transportation agencies in the United States” (p35). Therefore the need for an integrated asset management approach is apparent and, according to Anderson & Rivers (2013), recent recommendations have been made to change the focus from an “asset-by-asset approach to one that examines the entire corridor.”

Differences by transportation agency and asset type notwithstanding, many DOTs and agencies have adopted a common asset management approach, which has been dubbed the *worst-first approach*. This approach is simple: assets that have failed or have degraded to a state of disrepair are either repaired or entirely replaced (FHWA 1999). There may be two reasons why the worst-first approach is more common than a preventative approach: (1) tight budgets and limited funding require addressing the most critical assets, a reactive approach due to safety concerns, as opposed to spending the money on proactive measures; (2) justification to the general public for a proactive/preventative approach is difficult because the taxpayers expect the assets in the worst condition to be addressed first and that preservation is essentially interpreted as “fixing something that isn’t broken” (p21 FHWA 1999).

In lieu of these reasons, the worst-first approach has been deemed unsustainable. The FHWA admits that “most states limit application of their management systems to monitoring conditions and then plan and

program their projects on a worst-first basis" and that this approach is "tactical rather than strategic" (p16 FHWA 1999). Stanley & Pierson (2013) go one step further and claim the worst-first approach "results in overall system degradation as no assets receive preventative maintenance in time to keep the investment optimized" (p1660). So although a short-term fix of one failed asset may be cheaper, may receive more publicity, and is much easier to explain to the general public, it is actually much more dangerous and, on a longer timeframe, the worst-first approach is more time-consuming and costly than a preventative approach. Figure 1 shows a flow diagram of the processes involved in transportation asset management.

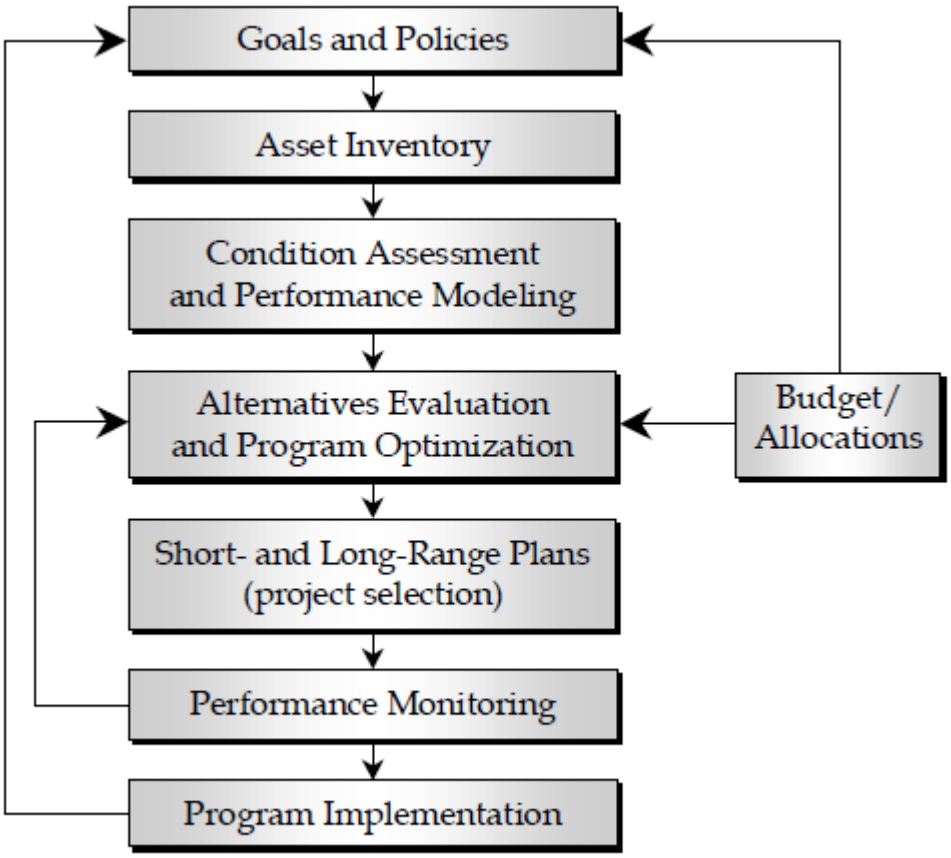

Figure 1. FHWA conceptual process diagram for transportation asset management systems. Taken from Cambridge Systematics, Inc., et al. 2002.

1.1.2. Geotechnical assets within the transportation asset management paradigm

Transportation systems include a wide range of supporting infrastructure. Among such infrastructure are all those elements that made of, or interact directly with the supporting ground, e.g. retaining walls, natural and cut slopes, embankments, foundations, etc. Such assets form a critical part of the transportation asset inventory and need to be included in the transportation asset management process. Sanford Bernhardt et al. (2003) define a broad set of geotechnical assets and show the importance of including geotechnical assets in the transportation asset management process.

A framework for geotechnical asset management was also presented, including the conceptual framework for a “geotechnical decision support system” by Sanford Bernhardt et al. (2003) and further expanded by Vessely (2013). A broad summary of generic goals and research needs for geotechnical asset management was given by Stanley (2011). Because it involves deterioration and potential failure of geotechnical assets as the driving factor, geotechnical asset management can also be framed from a risk management perspective (ARUP 2010). The asset management framework has been further explored for the specific cases of retaining walls (Anderson et al., 2008; Minnesota Department of Transportation 2013; Vessely et al. 2015), unstable slopes (Huang et al. 2009; Badger et al., 2013; Stanley and Pierson 2013), earth retaining structures (Brutus et al. 2009), embankments (Glendinning et al. 2009), slopes subject to rockfall (Rose 2005), and several other kinds of geotechnical assets.

A geotechnical asset management system needs to consider clear goals and policies set by the agency managing the assets (e. g. a State Department of Transportation). The goals are in general related to the quality and quantity of the service that they can provide to end users of the transportation system. Such goals may be difficult to frame in terms of the geotechnical assets themselves, but can be related to the overall performance of the transportation corridor, e. g. reduction in down-time of a road, or minimization of traffic congestions and travel delays due to lane closures. Following these lines, Anderson and Rivers (2013) propose a “level of service” approach to assess the impact of geotechnical assets on transportation system performance.

Fundamental to the asset management approach is the existence of a complete and well defined asset inventory. An inventory database should not only list all the assets, but describe any pertinent characteristics (e. g. dimensions, age, etc.), and most importantly, their state of performance, for it is through monitoring and tracking the state of performance that decisions about maintenance and repair can be taken, making the asset management process possible. Periodical updates are also necessary, and multi-tier approaches to the inventory have also been proposed (Vessely 2013). Several efforts to build asset inventories for particular types of assets can be found in the literature, for instance the efforts to

build extensive retaining wall inventories for geotechnical asset management purposes (DeMarco et al. 2010a and 2010b; Anderson et al. 2008; Brutus and Tauber 2009). In other cases, like those involving natural slopes next to transportation corridors, delineating the extent of what can be considered part of the assets may be challenging. Building such inventories will require efficient methods to capture and process large amounts of data. Our proposal is to use remote sensing data to help building such an inventory for slopes within the transportation corridor area of influence.

Central to the geotechnical asset management system is the performance monitoring and evaluations of the assets. This challenges in defining and operationalizing geotechnical performance standards has been discussed in detail by Vessely (2013), for assets in general, and by Stanley and Pierson (2013) specifically for slopes. A more detailed description of the needs related to this issue are given in the next section.

Other components of the geotechnical asset management system include analysis tools that will help in the decision making process, focusing on the potential of decreased performance and the risk of failure or even collapse of geotechnical assets (Sanford Bernhardt et al. 2003; Vessely 2013; ARUPA 2010). Such components, including a “decision support system” will also be considered in the project, and will be presented in other deliverables.

1.1.3. Performance monitoring of geotechnical assets

Defining the performance levels expected from the different assets, and devising a method for monitoring and repeatedly evaluating that performance, is key to the geotechnical asset management system (Sanford Bernhardt et al. 2003; Vessely 2013). The challenges of defining such performance levels and methods to monitor them has been described by several authors (e.g., Sanford Bernhardt et al. 2003; Vessely 2013; Stanley and Pierson 2013; Stanley 2011). Contrary to other types of assets (e.g., pavements, bridges, etc.), for which common engineering standards help define the expected performance and level of service over the life cycle of the assets, similar performance concepts can be harder to apply to geotechnical assets. Stanley and Pierson (2013) point out to the lack of understanding and data on the long term, life-cycle performance of geotechnical assets under different conditions of maintenance and external stressing conditions.

As any other service element, geotechnical assets are expected to deteriorate over time, but periodic maintenance and repair could help reduce such deterioration, and extend the lifetime of the asset. Performing maintenance and periodic repairs will have a cost, and estimating that cost versus the potential

costs of the asset's unattended deterioration may be difficult, such that the economic justification for spending money in maintenance and reparations will be challenging. Even defining the adequate level of maintenance can be a difficult task for geotechnical assets with a largely unknown behavior (e. g. natural slopes), especially when extrapolating into the future. The asset progressive deterioration through time can lead to an initially slow and later accelerating loss of performance, but it can also lead to a sudden, and often catastrophic failure of the asset, with consequences far beyond the economic loss of the asset itself.

Geotechnical assets will commonly involve a mass of rock or soil, as is the case of natural and artificial slopes, retaining walls, etc. Monitoring the state of the geotechnical asset may require expensive and complex testing and analysis, e. g. geotechnical core sampling, soil and rock mechanics testing, and computer numerical modeling of the stability of the asset. In some cases the cost could only be justified if there is a clear indication that a major and potentially catastrophic failure is likely. We propose a multi-tier approach in which remote sensing is used for monitoring geotechnical assets. At a large scale, low resolution remote sensing techniques are used to find priority areas that then are further investigated through higher resolution methods. Among the remote sensing methods, we propose a series of technologies that allow terrain deformation to be detected and measured at different time scales. Deformation of the terrain surface can be an indicator of the assets' health, as surface deformation may indicate progressive failure of the soil or mass rock. The magnitude, extension, and time history of the deformation can also give an idea of the magnitude and timing of a potential failure of the asset, allowing to gage the maintenance and repairing actions accordingly.

1.1.4. Ground movement and deformation as a key factor in performance monitoring

Slope deformation and landslide ground motion has been studied traditionally using in situ instrumentation (e.g., inclinometers and accelerometers). Measurements of direct variables, such as downslope displacement and/or velocity, and indirect variables, such as soil moisture content and ground water pressure, have been correlated to slope failure (Mikkelsen 1996). The installation and real-time observation of subsurface instruments would be the only way towards an attempt at forecasting landslides: sudden changes in precipitation amounts, groundwater pore pressure, or measured displacement rates generally indicate an increased potential for slope failure. This reactionary method of failure monitoring may work for slow-motion landslides where reaction times allow for mitigation

responses. In terms of quick-motion landslides, however, a negligible reaction time does not allow for any sort of anthropogenic reactionary measure and only leads to destruction. Therefore, proactive approaches have been generated in order to predict landslide failure in both the spatial and temporal sense.

A promising hypothesis was formulated by Fukuzono (1985) and further implemented by Voight (1989): there is a formulaic relationship between the strain applied to a material and that material's time of failure. This relationship was experimentally tested for metals (e.g., aluminum, nickel, and titanium) and soils (e.g., mixed mineral soil and Haney clay). The relationship discovered is as follows:

$$\Omega^{-\alpha}\Psi - A = 0$$

where Ω is the velocity, Ψ is the acceleration, and α and A are constants (Voight 1989). Time of material failure may be approximated by plotting the inverse velocity ($\Omega^{-\alpha}$) with respect to time. Material failure occurs when the inverse velocity approaches zero. The approximate time of failure is predicted to be the time at which $\Omega^{-\alpha} \rightarrow 0$. Figure 2 shows two scenarios where sets of inclinometer data located within the same landslide were converted into Λ measurements, where $\Lambda = \Omega^{-\alpha}$ (Petley 2004). Since $\Omega^{-\alpha} \neq 0$, applying a best-fit linear trend in the form Λ = mt+b -- where m is the slope, b is the Λ-intercept, and t is time -- solving for t yields the predicted time of slope failure. A linear Λ-t relationship has been observed in cases where brittle deformation or failure along pre-existing planes of weakness occurs (Kilburn & Petley 2003; Petley 2004). Nonlinear Λ-t relationships have also been observed (Figure 3) and have been interpreted as landslides exhibiting ductile failure mechanisms (Angeli et al. 1989; Petley et al. 2004; Petley & Petley 2004; Federico et al. 2012; Wartman & Malasavage 2013). Wartman & Malasavage (2013) found that predicting landslide failures using linear best-fit trend lines works better "with data collected closer to failure… but at the cost of reduced warning time" while nonlinear models "produce an excellent fit over the full time range of observed displacements" but requires "back-fit empirical parameters" which limits its application for landslide failure predictions (p 747).

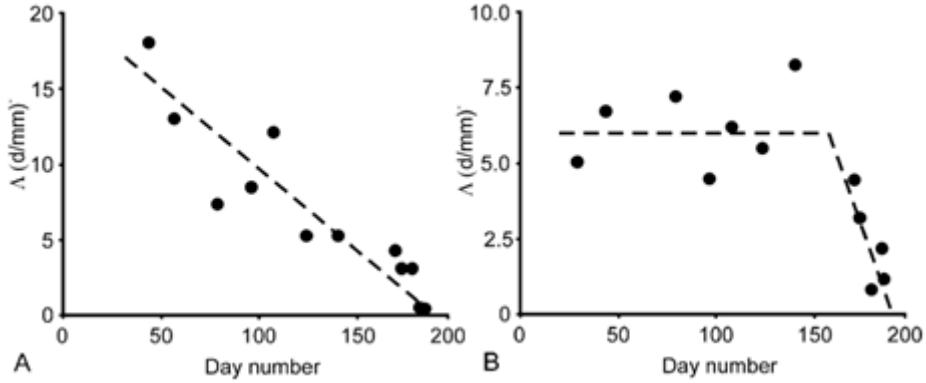

Figure 2: Λ-t plots of two inclinometers experiencing different deformation rates (Petley 2004). (A) Inclinometer experienced linear acceleration until failure at day 180. (B) Inclinometer experienced steady-state creep (horizontal trend line) until day 152 when a sudden increase in acceleration was observed until failure on day 180.

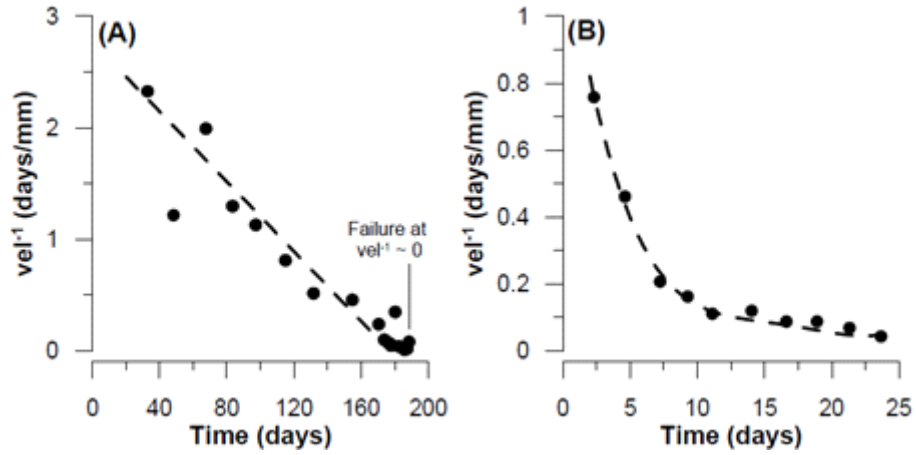

Figure 3: Λ-t plots of two inclinometers experiencing different deformation mechanisms (Wartman & Malasavage 2013). (A) Inclinometer displaying a linear trend indicating brittle failure. (B) Inclinometer showing a nonlinear trend indicating ductile failure.

1.2. Considerations for specific geotechnical assets

The general process described so far can be applied to a variety of different geotechnical assets. However, the peculiarities and particular characteristics of the different assets are important when tuning different methodologies for application to those assets. Some of these considerations are explored in the following sections.

1.2.1. Performance monitoring of slopes via terrain deformation

Slopes along transportation corridors may include a wide variety of types and origins. Depending on the material they are made of, slopes could comprise rock, soil, or regolith slopes, each with different failure mechanisms and deformation characteristics. Depending on their origin, slopes could be natural, artificial, or partially modified by human activity. Natural slopes may be less well known or characterized, but even engineering slopes can have a very complex behavior. Artificial slopes could be cut into the natural terrain, or built from filling material. Design and construction considerations should take into consideration the long term stability of the slopes, but sometimes those considerations are not effective in guaranteeing the long term stability of the slopes.

Terrain movement on a slope can have different implications depending on the slope characteristics and the nature of the movement. Movement of material at the surface of the slope, due to surface transport processes (e. g. erosion and deposition) may have little diagnostic value about the subsurface state of the slope, and the related stability of the material, but it may nonetheless be important for asset management practices.

Surface deformation can also reflect the movement along a deeper failure surface within the soil or rock body of the slope. Such a deformation can be used to infer a potential future collapse of the slope. Deformation patterns can be matched with modeled deformation and infer the possible size and extension of the failing area. The time history of deformation can also be used to infer the potential time of failure of the slope, as discussed in the previous section. Slope characteristics such as slope geometry (including slope angle and height), and slope material characteristics such as material strength parameters (e. g. friction angles and cohesion, for granular material, or fracture characteristics for rock masses), play a fundamental role in determining the slope’s stability and the observable surface deformation patterns. Steep and very high slopes on relatively weak material, may show less deformation before a major slope failure. Low rigidity or plastic materials may show large deformation without leading to catastrophic failure.

Moreover, total deformation will depend on the scale of the area that is deforming and therefore may lack physical meaning when considered at an individual location. Ideally, a measure of the deformation relative to the location of neighboring points, i. e. a measure of strain, should be considered when assessing the stability of slopes, but this may be difficult when low resolution remote sensing methods are being used. Large deformations varying slowly over a large area, may involve only small strains and

could therefore not be critical for the slope stability, whereas even moderate deformations that vary quickly over a small region could produce large strains, beyond the point of failure of the material on the slope. Strain is also physically related to the stress state within the slope mass, and such a stress-strain relationship is usually used to define the failure characteristics for the materials that make up slopes.

Slope stability and associated deformation will also depend strongly on external factors, especially those considered failure triggering events. Water pore pressure inside the slope, and its variations can play a major role in destabilizing the slope, and the long term presence of water also contributes with material weakening of the slope, through soil or rock alteration. Cumulative damage due to seismic activity acting on the slopes can also have a significant long term effect on the stability. Such long term effects could result in a reduction of the slope material strength, reflected in an increase of surface deformation observable through remote sensing techniques. But both seismic acceleration and interstitial water effects can be also very sudden, during high intensity events (e.g. earthquakes and extreme rainfall events), leading to slope failure without much warning. Such triggering events could cause slope failure without any warning observable through surface deformation monitoring.

Evaluating terrain deformation therefore needs to be done within the context of the particular type of asset, and the specific conditions under which it may fail, considering also the external factors that play into the slope stability and its deformation.

1.2.2. Performance monitoring of retaining walls via terrain and wall deformation

Retaining walls also include a wide variety of designs and field setups. In the case of retaining walls the two main areas to consider are the wall itself and the fill behind it, which the wall is designed to retain. Considerations about the backfill stability are similar to those discussed in the slope stability discussion, but the presences of the wall to provide support to the mass of soil acts to increase the stability.

Deformation monitoring may involve points on the wall itself or points on the backfill. Monitoring the deformation of the wall itself may be easier in the case of walls made of rigid materials (e. g. concrete), as the deformation (or straining) of a rigid material may be less and more predictable than that of the loose material contained behind the wall. Depending on the viewing geometry of the remote sensing technique used to monitor the deformation it may not be possible to directly monitor a wall or the backfill, but in

some cases the monitoring area may cover both. Monitoring the wall itself may also give results that are easier to interpret, as the deformation values could be compared with common engineering practices and standards for retaining wall deformation tolerances.

If deformation is measured on a large number of points along the retaining wall, and the wall geometry is relatively simple, it is also possible to model the wall as a rigid body and make much more precise measurements of displacement.

2. Remote sensing techniques for asset performance assessment and monitoring

Remote sensing techniques can be used to do different tasks as part of the geotechnical asset management process. Terrain models, including digital elevation models (DEMs) can be generated using remote sensing techniques; such DEMs can be used to characterize slopes near transportation corridors and do a first order classification of potentially problematic slopes, or slopes that may require further attention (e. g. more detailed characterization and monitoring). High resolution imagery can also be used to rate slopes according to their stability and potential for failure or producing rockfalls that may affect the transportation corridor. Such aspects have been discussed in other reports as part of this project. In this report we focus on ground displacement measurements from remote sensing instruments.

2.1. Ground displacement and deformation measurements using remote sensing techniques

A variety of techniques can be used to monitor geotechnical assets performance, and specifically to identify and measure terrain surface displacement. Techniques include Interferometric Synthetic Aperture Radar (InSAR), Light Detection and Ranging (LiDAR), and photogrammetric methods will be discussed in the following sections. Each of these methods can have a different instrumental platforms, including satellite, aerial, and terrestrial vehicles, as well as stationary platforms. Depending on the distance to the target and the instrument’s characteristics (e. g. focal length of the camera, scanning angle interval of the LiDAR instrument, or ground resolution of the InSAR images) a variety of resolutions or data-point densities can be achieved. Similarly, different methods can provide different accuracies, depending on instrument characteristics and platform setup.

2.1.1. InSAR

InSAR is a technique that utilizes data acquired as radar images in order to measure the phase shift between acquisitions. InSAR sensors are active, side-looking radar systems that transmit and receive radar waves. The sensors electronically record incoming radar echoes as complex numbers in the form of:

$$Ae^{i\Phi} = A\cos\Phi + iA\sin\Phi$$

where A is the amplitude and Φ is the phase of the radar wave (Dzurisin & Lu 2007). When multiple radar images are processed as a stack, the phase shift (ΔΦ) can be calculated at the pixel-scale relative to a reference image. The change in distance (Δd) between the sensor and any target pixel is calculated with the following relationship:

$$\Delta d = \frac{1}{2}\lambda\frac{\Delta\Phi}{2\pi}$$

where λ is the wavelength, the ½-factor is used to eliminate the two-way travel distance, and the quotient (ΔΦ/2π) represents the phase shift in fractional-2π terms.

There are two general processing approaches: two-pass interferogram generation and interferometric stacking. The purpose of generating interferograms (Figure 4) is to use the ΔΦ between two input images, where the total ΔΦ of an unprocessed interferogram may be expressed with the following relationship (Hooper et al. 2004):

$$\Delta\Phi = \Phi t + \Phi o + \Phi d + \Phi a + \Phi n$$

where Φt is the phase change due to topography, Φo due to orbital variations in the satellite path, Φd due to ground displacement, Φa due to atmospheric delays, and Φn due to inherent noise. The goal is to eliminate phase changes due to all factors except ground displacement. Two-pass interferometry is performed in subset of six steps: (1) image co-registration, (2) generation of complex interferogram, (3) application of a spectral shift, (4) common Doppler filtering, (5) interferogram generation with topography, and (6) interferogram flattening (removes topography). The resultant interferogram may be filtered and the coherence - “the ratio between coherent and incoherent summations” (Sarmap 2014) - is calculated. Interferometric stacking techniques, such as Persistent Scatterer Interferometry (PSI), is used to identify pixels within a stack of >20 input SLC images that consistently display high coherence values over a long period of time (Ferretti et al. 2001). These stable pixels are known as persistent scatterer (PS) points. Five general steps are included in the PSI workflow: (1) connection graph and area of interest definition, (2) interferometric process (similar to the six substeps listed in the two-pass interferometry process), (3) PS first inversion - calculates residual height, displacement, and velocity for found PS

points, (4) PS second inversion - models atmospheric effects based on spatial and temporal variations, and (5) geocoding.

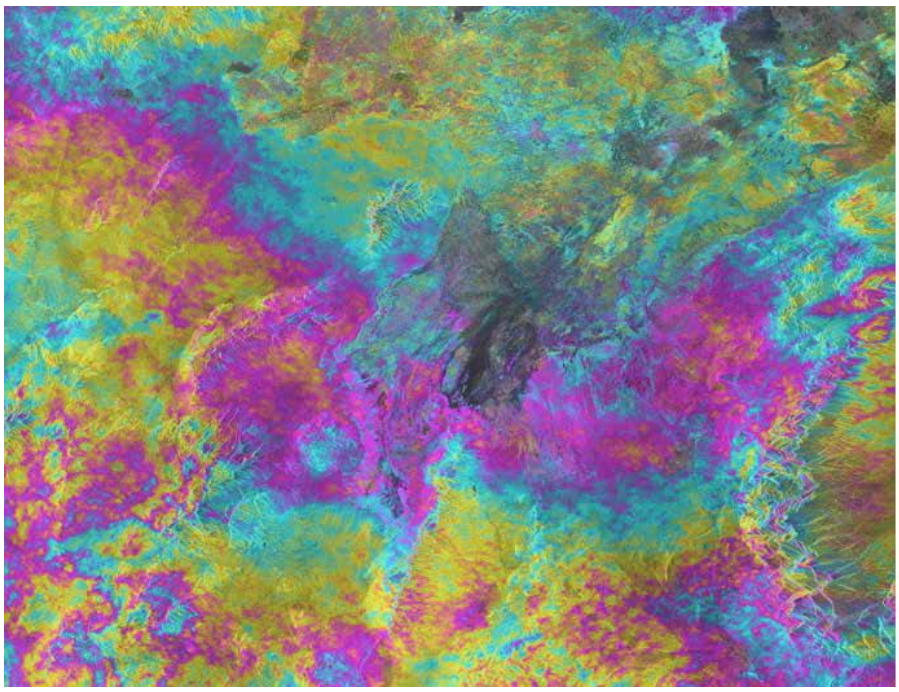

Figure 4: Example interferogram over the Salt Flats of Utah (Bouali et al. 2015).

2.1.2. LiDAR

LiDAR surveying techniques allow the generation of detailed geometric models of surfaces (Shan and Toth, 2008). Repeated applications of LiDAR surveys to such surfaces can create a time series of surface models, that when compared over time, can be used to derive surface displacements and deformations. LiDAR instruments produce intense light pulses (i. e. laser pulses) that are reflected back by the target surface and return to the instrument. By either estimating the time it takes for the light pulse to travel to the target and back (time-of-flight), or by comparing the phase of the emitted signal with the phase of the reflected signal as it comes back to the instrument, it is possible to estimate the distance from the instrument to the point on the surface where the light pulse was reflected back, this is also referred to as ranging. If the corresponding horizontal and vertical angles are measured for each emitted and reflected pulse, the reflection points on the surface can be located with respect the instrument, in a spherical coordinate system. Repeating this process many times (usually millions of times) a cloud of points with defined coordinates in space can be obtained, such a point cloud is effectively a sampling of positions on the target surface.

LiDAR surveys can be performed from mobile and static (terrestrial) platforms. Terrestrial LiDAR scans are usually more accurate, but will cover a smaller area and have a limited view of the target surface (single point perspective). Terrestrial LiDAR scans from several points can be combined to create a large point cloud, but the field deployment requires considerable labor. Alternatively, the LiDAR instrument can be mounted on a mobile platform, like a car, and point location acquisitions can be done as the platform moves, covering a much larger area that would be possible with terrestrial scanner deployments over a similar amount of time, but the continuous movement of the instrument introduces additional errors in the point cloud locations. To cover even larger areas, and from a sometimes more advantageous perspective, it is also possible to mount the LiDAR instrument on an aerial platform, and fly it over the target area. Usually, aerial LiDAR surveys can cover larger areas, but the point density (i. e. how many points fall per unit area on the target surface) and accuracy of the point locations is significantly decreased, compared with terrestrial LiDAR surveys.

The accuracy of the point positions will depend on the accuracy of the ranging (distance measurements) and the accuracy with which the horizontal and vertical angles are measured. Point measurement accuracies are usually in the range of a few mm to a 1 or 2 cm, and the relative error increases with increasing distance between the target surface and the LiDAR instrument. Accuracy considerations become especially critical for displacement measurements, because the errors in location can become artifacts in the displacement or deformation measurements. Point densities on the target surface depend on the angle that the surface forms with respect to the line of sight to the scanning instrument, but point densities of a few points per m^2 for aerial LiDAR, and densities of up to 10,000 points per m^2 for terrestrial scanners are common.

Using LiDAR survey point-clouds to measure surface terrain displacement also requires a high precision spatial co-registration of point-clouds from different times. This is usually done by choosing common tie-points that can be referenced to the same location in space, and it’s often fine-tuned using co-location algorithms like the “iterative closest point” (ICP) algorithm. Any miss-registration in the relative cloud-point location with respect to the other point-cloud could show up as an artifact in the displacement or deformation analysis; luckily such artifacts tend to be systematic in nature, relatively easy to spot, and sometimes to correct.

2.1.3. Photogrammetry

Photogrammetric methods that use stereoscopic reconstruction of the three-dimensional geometry of the terrain, based on two-dimensional photographs taken from different perspective locations, have been used since the early 20th century. Traditional methods made used of analogic instruments and operated usually on stereoscopic pairs of photographs. Recent developments in computer vision have allowed a series of photogrammetric algorithms, sometimes called “structure from motion methods”, to perform similar surface geometry reconstructions. Modern computer vision algorithms allow many overlapping digital images to be analyzed simultaneously, allowing for high image redundancy and diverse viewing geometry; the main advantage of this is the increase in precision and the versatility in using images from different perspective. The modern computer algorithms also transfer virtually the totality of the analysis burden from the user or analyst to the computer hardware and software, reducing costs and times of operation.

The output of such computer programs is either a point-cloud, similar to those produced by LiDAR scans, or higher end products, like DEMs and triangulated irregular surfaces (TINs). As with the LiDAR point-clouds, point-clouds generated through photogrammetric methods of the same surface at different times, can be compared to identify and measure surface displacements. And the correct co-registration of the point-clouds is also crucial to avoid artifacts in the surface displacement analysis.

2.2. Remote sensing surface displacement measurements techniques applied to monitoring specific geotechnical assets

Monitoring deformation of slopes and retaining walls using different types of remote sensing techniques is described and analyzed in the following sections.

2.2.1. Performance and monitoring of slopes using surface displacement analysis derived from remote sensing data

Terrain surface slopes of different types exhibit different displacement patterns, related to their internal deformation and potential failure modes. Varnes (1978) presented a classification of slope movement types and processes, which was recently revised by Hungr et al. (2014), describing different mechanisms behind each movement type. Deformation that may precede a slope collapse would most likely be associated to the “slide” type of movement, either translational or rotational. Other types of movements, like falls, and topples, are not expected to show significant precursory deformation, as they typically

involve smaller volumes of rock, and therefore correspond to smaller surface areas on the slope. Lateral spreads may show long term deformation that could be detected with remote sensing techniques, but it will depend on the direction of the deformation, as this would be expected to be mostly parallel to the slope, and acting on low angle slopes. Flows, if small, may show little precursory movement before the main failure, but small flows may not be as critical as larger flows either. Larger flows will likely start as major slope collapses, and those could show precursory movement that may be observable through remote sensing techniques.

Typical case slides will present very familiar patterns. Rotational slides should show deformation directed downwards on the upper part of the slide, and horizontally outwards, or even upwards movement on the lower reach of the moving mass. Such a pattern may be identified from remote sensing deformation measurements, if deformation measurement points have a high enough point density on the slope, e. g. with LiDAR or Photogrammetric methods. Satellite based InSAR may have a problem measuring deformation on enough points to be able to show such a distribution, unless specific conditions are met, such as the landslide area is extremely large or many anthropogenic structures are visible on the mass movement and the slide is not occurring too rapidly. This is especially the case for InSAR methods that produce sparse point coverage, like PS-InSAR. The directionality of the movement (downwards at the top, vs. outwards at the bottom) may also be difficult to tell with methods based on a single line of view approach (e. g. satellite based InSAR). Translational slope movements on the other hand, will show a more uniform direction, parallel and downwards with respect to the slope. Complex slope movements may be detectable if they are large enough and cover a wide area, but interpreting their potential failure mechanism can be challenging.

LiDAR and photogrammetric point-clouds could potentially be used to identify and measure slope movements on the order of a few cms. Applying a piecemeal ICP algorithm it is possible to recover three-dimensional displacement vectors from two point-clouds taken from the surface at different point. If the point density is high enough, it may be possible to characterize the movement type (e. g. rotational vs. translational slides). For falls or topples, the high density point-clouds may allow to reconstruct dislodged pieces from the slope that will either show up as missing pieces in the upper slopes, or as new pieces deposited on the lower slopes, after failure has occurred. Since the falls and topples process may be a longer term and more continuous process, this a-posterior approach may still be useful to assess the performance of the slope.

A first level of analysis with respect to deformation would be to identify all those slopes that are showing some kind of deformation. For methods that cover large areas, like InSAR, this is a first screening for potentially critical sites. Slopes that are also identified as potentially unstable through other means (see next section) but show no InSAR deformation, may need to be analyzed with other remote sensing methods to look for smaller scale deformation. Once a deformation has been identified, measuring it (how big is the deformation? what area does it cover?) and estimating the associated strains would be the next step of analysis. The velocity and acceleration trends of the movement could also be incorporated in the analysis, if there is a complete enough time series allowing for this.

Performance indices derived from displacement measurement need to also consider other slope characteristics, such as slope material, geometry (e.g. slope angle and height). This can be done by incorporating the deformation information as part of a broader slope performance rating scheme, we show how this can be done in the next section.

2.2.2. Performance and monitoring of retaining walls using surface displacement analysis derived from remote sensing data

Deformation of retaining walls shares some similarities with that of slopes, but can be fundamentally different in many ways. Retaining walls tend to be vertical or sub-vertical, and can be subject to large lateral forces, which will tend to produce a later outwards displacement of the wall. The backfill may show settlement associated to this process, but it may also settle in a natural way, especially shortly after the wall construction (Clayton et al. 2013). But other rigid failure modes are also possible, including overturning, bearing capacity failure, and global instability (Ashmawy, 2013). Such failure modes would exhibit very particular types of deformation, that, given a high enough density of measuring points on the wall, could be easy to recognize from the measured deformation pattern. Non-rigid types of movement could also happen on flexible walls (e. g. steel-reinforced type), and the corresponding deformation patterns measured through remote sensing methods can be much more complex (Clayton et al. 2013; Ashmawy 2013). Fitting of plane or curved (e. g. polynomial) surface through the deformation measurements can help elucidate such complex deformation patterns.

A certain amount of displacement may have been considered as tolerable in the wall design, especially for lower rigidity structures, but large deformations will usually imply performance degrading or even failure of the wall system. Defining those levels of deformation deemed unacceptable may be something that the

agencies in charge of the geotechnical asset management system will have to do, according to the asset's design and other similar criteria (Clayton et al. 2013; Ashmawy 2013).

3. Multi-tier approach to geotechnical asset performance assessment and monitoring

Geotechnical asset performance monitoring can be done at different levels, depending on the scale and detail of the features being monitored. Here we describe a multi-tier approach that makes used of different remote sensing datasets, at different scales and resolutions. There tends to be an inverse relationship between the spatial extent and the resolution of remote sensing data, datasets covering large areas are easier to produce at lower resolution, whereas high resolution datasets are usually only feasible for smaller areas. We exploit this feature by proposing a multi-step analysis, in which large areas are analyzed first at lower resolution, to recognize areas where more detailed analysis may be necessary.

3.1. Considerations on the scale, resolution and detail of the information and analysis.

Transportation corridors can be extensive, spanning over lengths of thousands of kilometers, but the issues affecting geotechnical assets along those transportation corridors may be subtle, and in the case of deformation, may be measured on the scale of millimeters. This range of length scales presents a significant challenge for monitoring geotechnical assets, and it's further complicated by the time recurrence at which some of these datasets may be need to be meaningful for monitoring purposes, e. g. monitoring of a fast moving slope may require frequent measurements of displacement, especially when the slope approaches the state of failure.

To address these challenges, we propose the use and merging of a suit of different datasets and methods, at each level of analysis. Low resolution and large scale datasets generated through different methods, including public-access and freely available datasets related to surface terrain topography (e. g. DEMs) can be used at a first level of analysis to identify steep and high slopes that may be more critical to analyze. Other datasets describing the broad characteristics of the slopes, like the geology of the soil coverage could further be used to assess what slopes require a more detailed analysis. Information about potential triggering events, like seismic hazard maps and recurrence probability maps can also be incorporated in this analysis. The exact details of how such information can be integrated may depend on

the criteria of the analyst, in the following sections we show how some of these datasets can be incorporated for the analysis of slopes along a railroad corridor.

Few displacement methods can be applied over very large areas and give highly precise results, however satellite based InSAR is capable of doing this. Each InSAR scene can cover thousands of square kilometers and produce displacement values of a few millimeters. The main limitation with this methods is the data point density in some cases. Sparse point coverage may miss important slopes on which movement is happening but coherence is low to produce a meaningful displacement estimate, sometimes because the displacement is so high that the coherence breaks down. For these and other reasons the displacement value alone at this level can't be the only criterion to identify critical slopes.

High resolution datasets for specific areas are in general not available in the public domain, and will have to be collected for the specific goals of geotechnical asset monitoring, once smaller, high priority areas have been defined in the previous analysis. LiDAR and Photogrammetric methods discussed in previous sections can be used to generate high resolution and high accuracy geometric representations of the slope terrain, either in the form of point clouds or DEMs. Such high resolution terrain representation generated repeatedly over time can also be used to monitor displacements, and if they overlap with InSAR measured deformation, the results can be compared and validated.

Geotechnical asset monitoring through remote sensing techniques, and the corresponding performance estimations are limited to how the data collected from three-dimensional surface geometry reconstruction and surface displacement data, can be interpreted in terms of the assets performance. Once the remote sensing derived analysis shows that a slope may be moving and it's geometry is critical (very steep and high), the next level of analysis may be required, including geotechnical modeling of the slope's stability, the initiation and propagation of slope failure or collapse scenarios, and their potential impact on the transportation corridor assets and general performance. For all but the simplest cases, this will require additional data that cannot be provided through the remote sensing analysis, e. g. soil or rock material properties, and at that point the analysis becomes a traditional geotechnical one, for which the remote sensing data can still be very valuable, but are not sufficient.

Seen in such a context, the remote sensing data described in this report allow to focus attention on geotechnical assets in critical areas, and if needed perform more in depth geotechnical studies of those assets. The assets performance at early stages of deterioration can be inferred from the remote sensing data, but later deterioration (e. g. close to failure) stages may require more in depth geotechnical

evaluation. This is similar to the use of (and actually can make use of adapted versions of) visual inspection methods, like the “Rockfall Hazard Rating System” (Pierson 1992, 1993). The following sections describe the remote sensing datasets that can be used at different scales for the purposes just described.

3.1.1. Large scale, wide coverage datasets and their analysis

Identifying the slopes that are most critical to monitor from a geotechnical asset management perspective is the first step of the monitoring process, particularly in relation to their stability and the impact their instability could have on the transportation corridor. Slopes along transportation corridors range from small (a few meters high) cut and fill slopes along gently sloping terrain, to large (hundreds of meters high) natural slopes on steep, high-relief, mountainous terrain. Slope material can range from loose soil or regolith type material, to solid rock, with the material strength varying accordingly. Slope angles vary from relative relatively low (< 20 º) for less resistant slopes to virtually vertical, for highly competent rock. The maximum slope angle formed by low cohesion granular material, will be controlled by the material's angle of repose, which usually is around 30º to 35º; but cohesion, and tensile strength in general, can increase the slope angle to high values. The higher the relief of a slope and the higher its angle, the less stable it will be, therefore high and steep slopes are less likely to remain stable for a long time.

Long term stability of natural slopes also depends on other factors, like the frequency and intensity of triggering factors, including seismicity and rainfall, the presence of erosive forces (e. g. fluvial erosion at the base of the slope), and the direct action of tectonic deformation, e. g. faults directly acting on the slope. Some of the processes underlying slope instability are also processes that drive terrain relief rejuvenation in the first place, leading to the formation of high and steep slopes; e. g. tectonic activity, particularly tectonic uplift and similar orogenic processes. Therefore, as a general rule, regions of high tectonic activity will tend to show the steepest and highest slopes; and such slopes will tend to be less stable, collapsing and failing more often on the long term.

Relief and slope steepness therefore can be used as a proxy for relative slope stability due to the direct physical mechanism behind slope failure and collapse, but also because of its correlation with other factors (e. g. external triggers) that are also related to slope stability. High relief and steep slopes correlate with relatively unstable areas, that are frequently collapsing, and are far from a state of equilibrium;

whereas low relief and low slope angles correlate with relatively stable areas, at which the topography as reached a certain degree of equilibrium.

The previous considerations have not included the impact of human activity on slope stability, especially the direct impact of transportation corridor construction and slope modification work (e. g. cutting slopes). Such impacts could be significant, including cases of slopes that under natural conditions would be relatively stable and close to an equilibrium state.

The impact of a slope's stability on the transportation corridor will also depend on how close it is located with respect to the corridors' assets. Transportation corridors located on large sloping terrain will inevitably be close to the slope, but corridors located at the bottom of wide valleys or at the top of topographic plateaus, may be further away from significant slopes. As the definition of the slope is not just a binary classification, but a continuous range, depending on the slope angle and the slope height, measuring the distance to a significant slope may not be a very straightforward process. The slope angle and the height-over-length approach explained later in this document is one approach that can be followed for this purpose.

Taking all these factors together and considering those variables that can easily be assessed from remote sensing data, we can focus our analysis on two main variables, slope angle and slope height, and these two variable scan be analyzed jointly to identify what sections of the transportation corridor could be most critically affected. Large scale datasets containing this information include DEMs that cover the entire United States at different resolutions. DEMs with a 10 m pixel resolution cover the majority of the contiguous States, and 1 arc second (~ 15 - 30 m) pixel resolution DEMs have a worldwide coverage. Slope angle and slope height calculated from 10 m DEMs will be appropriate for slopes that are at least several tens of meters high, over horizontal lengths of at least a few hundreds of meters. Such slopes are the highest priority targets in rugged terrain areas, as discussed previously.

In the absence of other variables, slope angle may be the single most important variable determining slope stability. Although a multi-category classification could be applied, used several values of slope angle to rank their stability, here we will use a binary classification with a single threshold value separating critical slopes (or slopes of interest) from other slopes. The choice of a threshold slope value is somewhat subjective, but noting that the repose angle for non-cohesive granular material is usually near to 30º, we can use this value as a first guess for our slope threshold value. If more detailed information about slope

stability and angles was available, e.g. from a landslide or slope instability catalog of map, that threshold value could be adjusted accordingly.

The slope angle criterion helps identify areas where the slope may become unstable and a potential slope collapse could initiate, but the actual impact on the transportation corridor may depend on whether the failure or collapse actually reaches the transportation corridor infrastructure or assets. If the potentially unstable location is within the corridor area of interest, no further consideration may be necessary at this level of analysis, as the location would automatically be considered of interest for further analysis; if on the other hand the potentially unstable location is outside, but near the transportation corridor, it becomes necessary to analyze how likely it is that such an instability could propagated to, and affect the transportation corridor.

At a first level, a wide buffer zone (e.g. 1 km width) can be generated around the transportation corridor, to focus the analysis on a narrower zone. This implies that any slope instabilities outside of the buffer zone are judged to not have any effect on the transportation corridor. The choice of the buffer width therefore will reflect our estimate of the farthest distance that potential slope failures or collapses can travel, e.g. as a landslide. Runout distances for different types of mass movement can vary considerably, from relatively short for small landslides, to very long for debris flow type of mass movements. Extremely mobile types of mass movements (e. g. debris flows) may require a different type of analysis, and will usually also be confined to particular paths and locations (e. g. drainage channels or alluvial fans and planes). The width of the buffer zone will also depend on the height of the relief, as the higher the relief of the unstable slope is, the longer the potential runout of a landslide can be, as will be discussed in the following paragraphs, when discussing the H/L criterion. Importantly, if the areas flagged as critical in the H/L analysis reach the boundary of the buffer zone, it may be necessary to extend the width of the buffer.

The runout distance reached by a sliding mass, quantified by the horizontal distance traveled (L) will depend on, among other variables, on the elevation drop of the collapsing material (H), and the ratio H/L can be used as a mobility parameter for a slide (Hsü 1975; Corominas 1994; Finlay et al. 1999; Hunter and Fell 2003); the lower the H/L ratio, the longer the runout distance the sliding mass will reach. The value of H/L may depend on different factors, most notably it is strongly correlated to the collapsing mass volume: larger volume slides usually have lower H/L values. Other variables affecting the H/L ration include the slide material properties, most notably the presence of water or other fluids that could significantly increase the runout distance, as noted before; excluding those cases from the analysis (and

noting that they require a separate analysis) one can focus on a narrower set of slide types for which a reasonable range of H/L values can be estimated.

For small to moderately large slides ($<10^5$ m^3) the H/L values are usually in the 0.2 to 0.5 range (Corominas, 1994; Finlay et al., 1999; and Hunter and Fell, 2003), whereas larger slides (up to 10^9 m^3) can have H/L values as low as 0.1 and lower. Choosing a particular H/L ratio can be done, either based on knowledge of the local characteristics of the landslides (e.g. through a landslide catalog or map) or based on the global averages, but considerations on how conservative the required safety level have to bee also play into the choice. For the example presented in the second part of this report we use a 0.5 value for the H/L ratio threshold, which corresponds to smaller volume slides.

For a given H/L ratio threshold and a set of possible initiation points, the areas within reach of landslides can be mapped using the DEMs topography (e.g. Jaboyedoff et al. 2005; Jaboyedoff and Labiouse 2011). In our example discussed in the second part of this report, the initiation points are all the points (pixels in the DEM) with a slope larger than the threshold slope (30º for our example). For each of those points (pixels) it is relatively easy to calculate all the pixels in the DEM that are below a line with a slope value equal to the H/L threshold. The set of all the lines with a slope equal to H/L that pass through a given point (the landslide origination point) form a cone with an H/L slope, the intersection of the cone with the DEM surface defines the area within reach of the landslide propagation.

After calculating the cones for all the initiation points it is relatively easy to map all the pixels that fall within a cone. Moreover, it is possible to count how many times each pixel falls within a cone, pixels that fall within many cones could be exposed to landslides from many different sources, and in that context the number of cones that reach a pixels become a proxy for the pixel’s exposure to landslides from different sources. This information can be used to do a relative ranking of the hazard exposure, and include it in the selection of critical slopes.

In this way, using a 10 m pixel (or 30 m pixel in some areas) DEM, and considering a buffer zone around the transportation corridor, one can identify critical pixels that may be at a relatively high risk of collapse due to the slope angle. Applying the H/L cone mapping procedure, it is further possible to identify the areas along the transportation corridor that could be exposed to possible landslides that originate somewhere else but for which the corridor is within the runout distance. Additionally, in some cases, measured slope displacement can also be incorporated in the analysis, through InSAR measurements.

InSAR displacement values are obtained from converting phase shifts from interferograms created from two or more radar images of the area of interest; when there is high spatial coherence for all the pixels within a certain region, a displacement value can be assigned to each of those pixels, but when coherence is low, like on highly vegetated areas, the phase shift cannot be converted to displacement as easily. In such cases, other techniques, like PS-InSAR, which uses a large number of images, can be applied even if there is not high coherence between all pairs of pixels across two images, producing a sparse set of points with displacement information. Such a set of points can be very useful, but the sparse nature of the point-dataset results in missing information due to image pair decorrelation. It also means that even when a few points can be retrieved for a slope, the point density (usually only a few points over several thousand square meters), will not allow for a detailed reconstruction of the spatial pattern of displacement (e.g., interpolation). In this case, it is necessary to rely on other methods to obtain such detail.

3.1.2. Intermediate to small scale, narrow coverage datasets and their analysis

The next level of analysis requires the collection to intermediate to small scale, and narrow coverage datasets, at a much higher resolution (or data-point density). Two remote sensing methods are considered at this level as part of this project; LiDAR and photogrammetry. These methods produce point-clouds representing the three-dimensional geometry of the slope surface, each point-cloud can contain tens of millions of points, and each point can have a relative precision on the order of a 1 – 2 cms. Collecting and comparing such point clouds over time allows to track the surface changes, including the changes associated to slope surface deformation or displacement.

Acquisition platforms include terrestrial static, mobile (from a vehicle, like a car), and aerial (either from a plane or from an unmanned aerial vehicle (UAV)). The longer the distance between the data acquisition instrument and the target surface is, the lower the resolution of the resulting dataset will be, but the area covered in a single acquisition campaign will be larger. Such an inverse relationship between the dataset resolution and the areal coverage translate in a trade off between the amount and quality of the collected data (i. e. the resolution), and the cost or resources used to collect the data (more overflight passes, a larger number of scans, etc.). The right balance between the needs for information and the cost in obtaining that information has to be achieved, and will vary from case to case, depending on the specific needs and resources available to the user.

Aerial data collection from conventional platforms (e.g. airplanes) will usually have a longer instrument to target distance, but will provide quick coverage of large areas, such datasets could be considered of intermediate resolution. Data collected from static positions or from low flying UAVs will produce much higher (one to 4 orders of magnitude) resolution or point density datasets, which would fall into the high resolution category. The cost of collecting such data, per unit area of the target surface needs to be justified for the collection of such high resolution dataset. Justice (2015) shows how very high resolution datasets can be incorporated into the slope stability analysis, in comparison with low resolution datasets (e. g. 10 m pixel DEMs). For instance, geotechnical modeling based on numerical methods, for a slope of a few tens of meters in height, requires slope profiles at a much higher resolution than those that can be extracted from a 10 m pixel DEM; for such cases a data point density > 1 point per meter is ideal. Traditionally such profiles require field surveying campaigns over sometimes difficult access areas, but the output of the remote sensing methods produces high quality profiles, with a much higher point density that those produced from surveying campaigns.

High resolution point-cloud data can also be used to characterize the texture and surface structure of the slope. Rock slope textural features, like joint-set orientation and density, faulting and shear zones can also be interpreted from the high resolution point clouds. Moreover, many LiDAR instruments and all photogrammetric methods produce visible color spectral information for the target surface i. e. the color of photographs taken from the surface, usually in the form of 8-bit values for the red, green, and blue (RGB) bands of the camera sensor (e.g. CMOS or CCD). Such color information can also be incorporated in the texture of structural analysis of the slope surface. In the case of LiDAR instruments, small collimation differences between the photographic camera optical axes and the LiDAR beam may result in small misalignments between the points' location and their corresponding colors, which can result in less precise interpretations of the texture or structure.

For soil and rock slopes, the analysis of clasts sizes can also be done from the high resolution, RGB point-clouds, especially for larger (larger than several cms) fragments. This can be particularly useful in characterizing the slope for rockfall hazard rating purposes (Pierson 1992, 1993). Justice (2015) and Bouali et al. (2016) have shown how such data can be used within rockfall hazard rating systems that require information on the sizes of the largest clast that fall of the slope.

Displacement or deformation analysis from high resolution point-clouds provides one of the most informative outputs at this level of analysis. Once point-clouds from different times have been generated and co-registered to a common coordinate system, such that the slope surface areas that have not change

over time coincide spatially, the displacement analysis can be done. Displacement analysis methodologies range from the simplest and computationally most efficient (e. g. raster elevation (DEM) differences) to more sophisticated, three-dimensional displacement vector algorithms.

For cases where the displacement happens mainly in one direction, or the interest is mainly in unidirectional displacement measurements, e. g. a relatively low angle slopes subject to settlements or movements that are mainly oriented perpendicularly to the surface of the slope, a unidirectional displacement analysis based on raster differencing may be satisfactory. In this type of analysis the point locations in three-dimensional space are reduced to a two-dimensional matrix of values (i. e. a raster dataset), with the third dimension given by the values stored in the matrix elements. This is done by choosing a two-dimensional planar coordinate system embedded in the three-dimensional space, and oriented such that the direction of interest for monitoring the slope movement is perpendicular to the plane coordinates system. The perpendicular distances from the points to the plane in three-dimensional space then become the variables of interest. A grid or regularly spaced points on the plane is then defined, and the values of the surface represented by the cloud point is then interpolated in two-dimensions for the locations of the regular grid, using a two-dimensional interpolation algorithm. When the two-dimensional plane coincides is horizontal with respect to a local coordinate system, the interpolated raster is a DEM.

Once two or more distance (or elevation, in the case of DEMs) rasters have been generated, such that their pixel positions align exactly, the distance or elevation values can be directly subtracted on a pixel by pixel basis, resulting in a new raster of distance or elevation differences, which would correspond to the displacement or deformation of the surface in the direction perpendicular to the raster. Using this method with successively generated DEMs, we can track vertical changes on a slope. And the results can be further extended to analyze displacement components parallel to the surface, by exploiting the fact that for small deformations or strains, a surface with enough vertical relief can locally preserve the correlation properties between elevation values for DEMs of different times. The apparent shift in topographic features needed to match the elevation values locally, can then be interpreted in terms of displacements parallel to the raster plane.

A fundamentally similar idea of correlation feature shapes and positions at a local scale, can also be applied directly to the three-dimensional point clouds from different times. The complexity of the algorithms involved in this task is however much larger than for the raster correlation. Piecemeal application of algorithms such as ICP. can give good results. An additional advantage of directly using the original three-dimensional point clouds is that tree components of translation and tree components of

rotation can be obtained for each local set of points, i. e. displacement and rotation vectors can be calculated for subsets of points. The accuracy of these techniques depends on the accuracy of the original point-clouds, but also on the number of points in the subset used for each local correlation; for low point density datasets this may be a limitation. Conversely, a larger area can be chosen, but that will result in less points for which we will be able to calculate movement vectors. The texture (i. e. local spatial variability) is also an important factor; relatively smooth surfaces will be harder to correlate locally.

The second part of this report shows an example of how such datasets can be applied to a transportation corridor. In the case of those examples, LiDAR was collected from static terrestrial positions, and images for photogrammetric analysis were collected from a UAV.

3.1.3. Detailed geotechnical characterizations and studies, beyond the remote sensing analysis

Once the characterization of a slope based on remote sensing and other non-contact methods has been done, the results of the analysis may be inconclusive as to the state of the asset and the actions that need to be taken. In such cases, more detailed geotechnical analysis and perhaps modeling may be necessary. Discussing the generalities of such a level of analysis goes beyond the scope of this report, but it is important to mention that the data generated from the remote sensing methods, like high resolution DEMs (and their derived products, like slope and aspect rasters) and point-clouds may be a vital input to more sophisticated geotechnical analysis methods. As mentioned previously, Justice (2015) and Bouali et al. (2015) have presented some examples of such applications. The second part of this report will also illustrate such a use of the remote sensing data.

3.2. Multi-tier hierarchy of analysis

The description of a multi-tier analysis process in previous sections of this report can be synthesized in a hierarchical process, where inputs at different levels of analysis produce outputs that are ingested in the follow analysis level, in a progressively more detailed, more focused, and narrower process. At each level the analyst must consider if the information produced is necessary to make a decision about the geotechnical asset management, the information outputs can be categorized in three broader types. First, if the analysis indicates that the assets is not showing any signs of deterioration or loss of performance (e.

g. the possibility of failure or collapse of a slope), the asset does not require further consideration for now and the analysis process for that asset ends at that point, with the caveat that this decision may change in a future round of monitoring.

In the second type of output, the analysis shows that the asset could be in a critical state in which deterioration and loss of performance is likely, but the current level of analysis is either not certain enough about such a state, or it is not conclusive about the course of action to take to mitigate the deterioration, repair or maintain the asset. This type of output points to the need of doing a more in depth analysis, which corresponds to next level of analysis, in order to either determine with more certainty the state of the asset, or to analyze the course of action or intervention to avoid a significant loss of performance (or even catastrophic failure or collapse) of the asset.

The third type of output focuses on the diagnostic of the geotechnical asset state, and the possible actions that are required to avoid a loss of performance, or even failure or collapse of the geotechnical asset, and other assets it supports. The detailed discussion about this type of output is outside the scope of this report, and falls within the more specific type of analysis and decision making in geotechnical engineering, but it may use some of the outputs produced by the other levels of analysis, and is therefore relevant to the whole hierarchical structure of the monitoring system.

The process is illustrated by the diagram shown in figure 5. The different levels of analysis, their respective remote sensing inputs and information outputs, and the associated decision types are shown schematically. Justice (2015) developed a more specific prototype of the hierarchical process, for a case study of a rock slope along a railroad corridor. Bouali et al. (2016) further adapted the process taking the conceptual framework of the rockfall hazard rating system originally proposed by Pierson (1992, 1993), to incorporate some of the remote sensing output products into the analysis, most notably the slope surface deformation or displacement. The second section of this report describes such a study case in more detail.

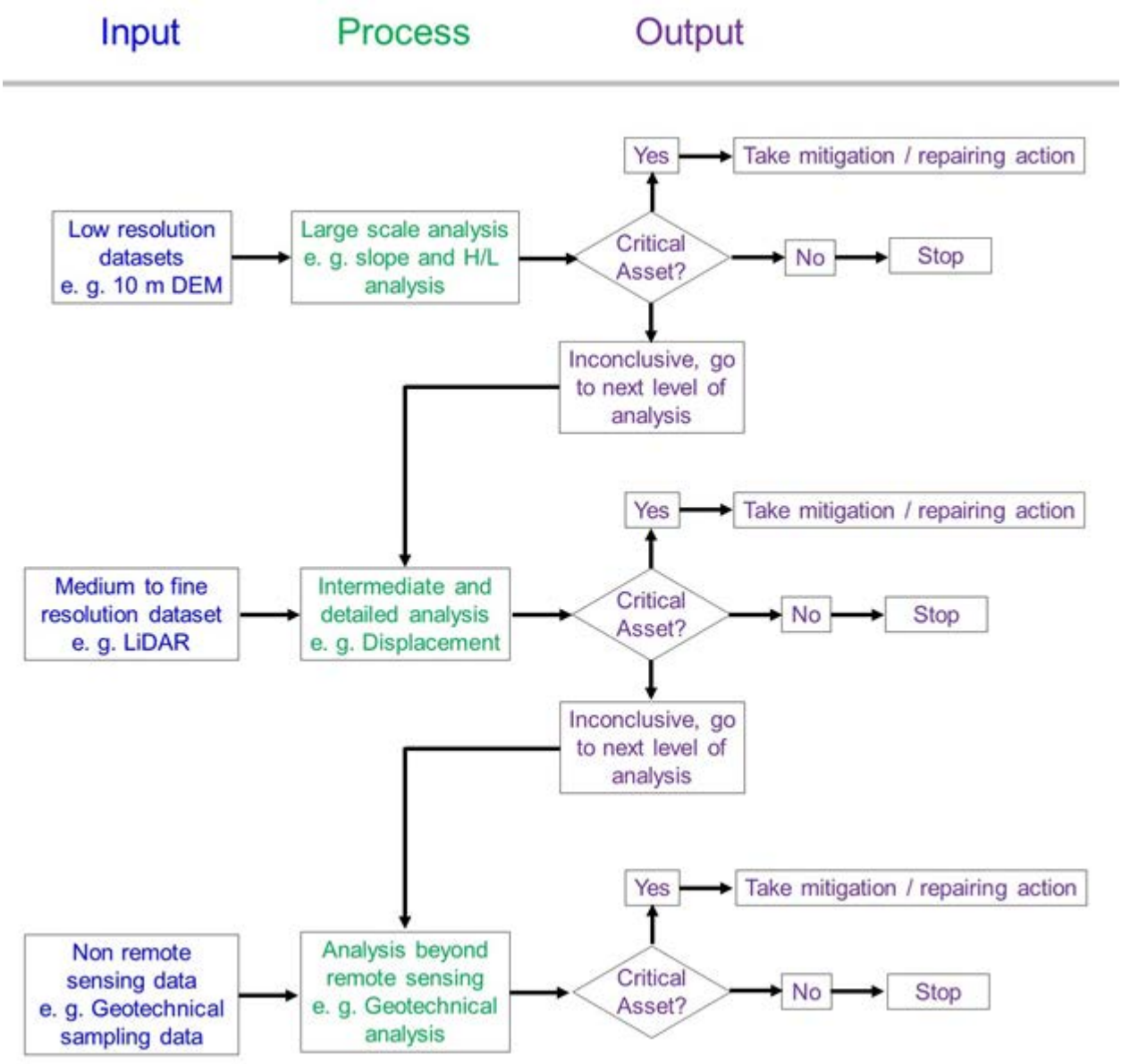

Figure 5. Flow diagram illustrating the multi-tier analysis process proposed for monitoring geotechnical assets.

Deliverable 4-B

4. Study case examples to demonstrate the performance modeling of geotechnical assets using remote sensing inputs: A geotechnical asset rating tool

In this section we present two study cases on the application of the remote sensing techniques described in previous sections of the report. The first study case is on slopes (natural and human altered) along a railroad corridor. The second study case considers retaining walls along a major highway in an urban environment. Much of this work was done as part of Masters and Ph D projects that have been published or are in the process of publication, especially the works by Justice (2015), Cerminaro (2014), and Bouali et al. (2016).

4.1. Slopes along a railroad corridor in Nevada

The Nevada study site is a railroad transportation corridor that follows the low valley topography of a canyon system. Slopes of varying degrees of steepness (e.g., near-vertical to gently dipping) are located along one or both sides of the route along many segments of the tracks. Most of the slopes are composed of volcanic rock, such as rhyolite and tuff, as well as metamorphosed welded tuff-breccia with basalt-capped plateaus upon the tallest slopes (Bouali et al. 2016).

The following subsections focus on two scales of analyses. The large scale analysis examines the railroad corridor as complete network and, more specifically, studies a 29-km portion of the railway (Figure 6). The intermediate and detailed scale analysis examines individual transportation and geotechnical assets (e.g., slopes) within the railroad corridor.

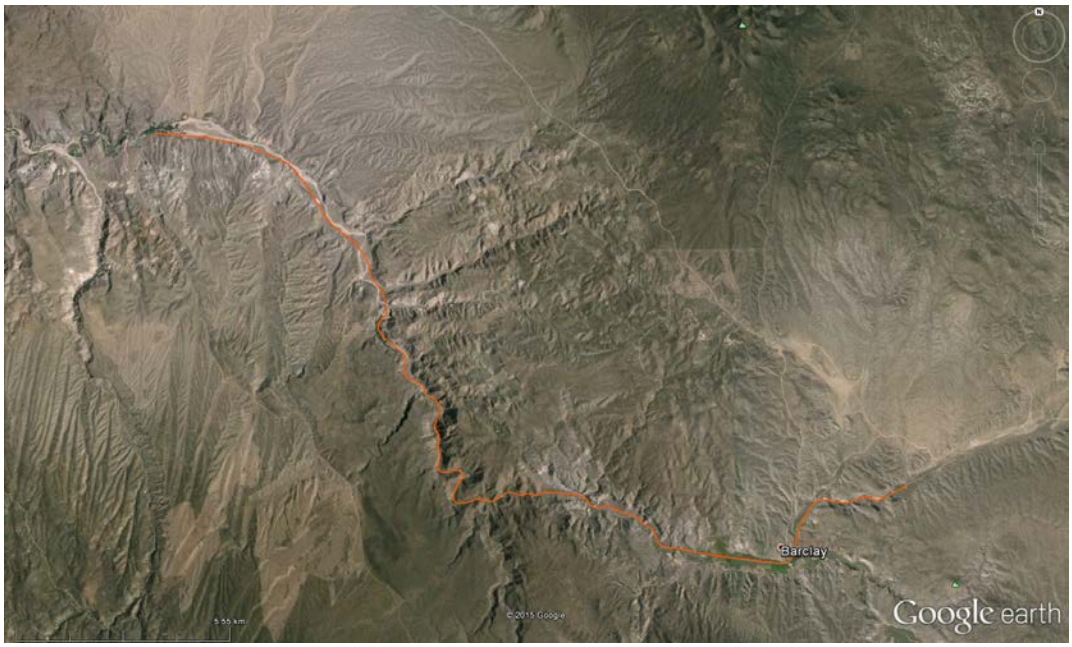

Figure 6: Large scale analysis of 29-km segment of railroad corridor (orange) in southeastern Nevada.

A railroad corridor in Nevada is used as an example of multi-tier geotechnical asset monitoring methods previously discussed, and the slopes in its area of influence are the asset type considered. The terrain relief along the corridor ranges from relatively gentle, on hilly terrain inside a broad valley, to very steep, on highly incised and narrowly confining canyons. Slopes include both natural, artificially modified (e. g. cut slopes) and mixed type slopes. The corridor stretch is dominated by rock slopes, mainly formed in welded ignimbrites, but some less competent materials, like partially cemented alluvium and regolith also form some of the slopes.

4.1.1. Large scale analysis

The first step of analysis is to look at the entire stretch of corridor and analyze what sections may be inside the area of influence of potentially critical slopes. We define a 1 km buffer area around the railroad track as the potential influence area (figure 7).

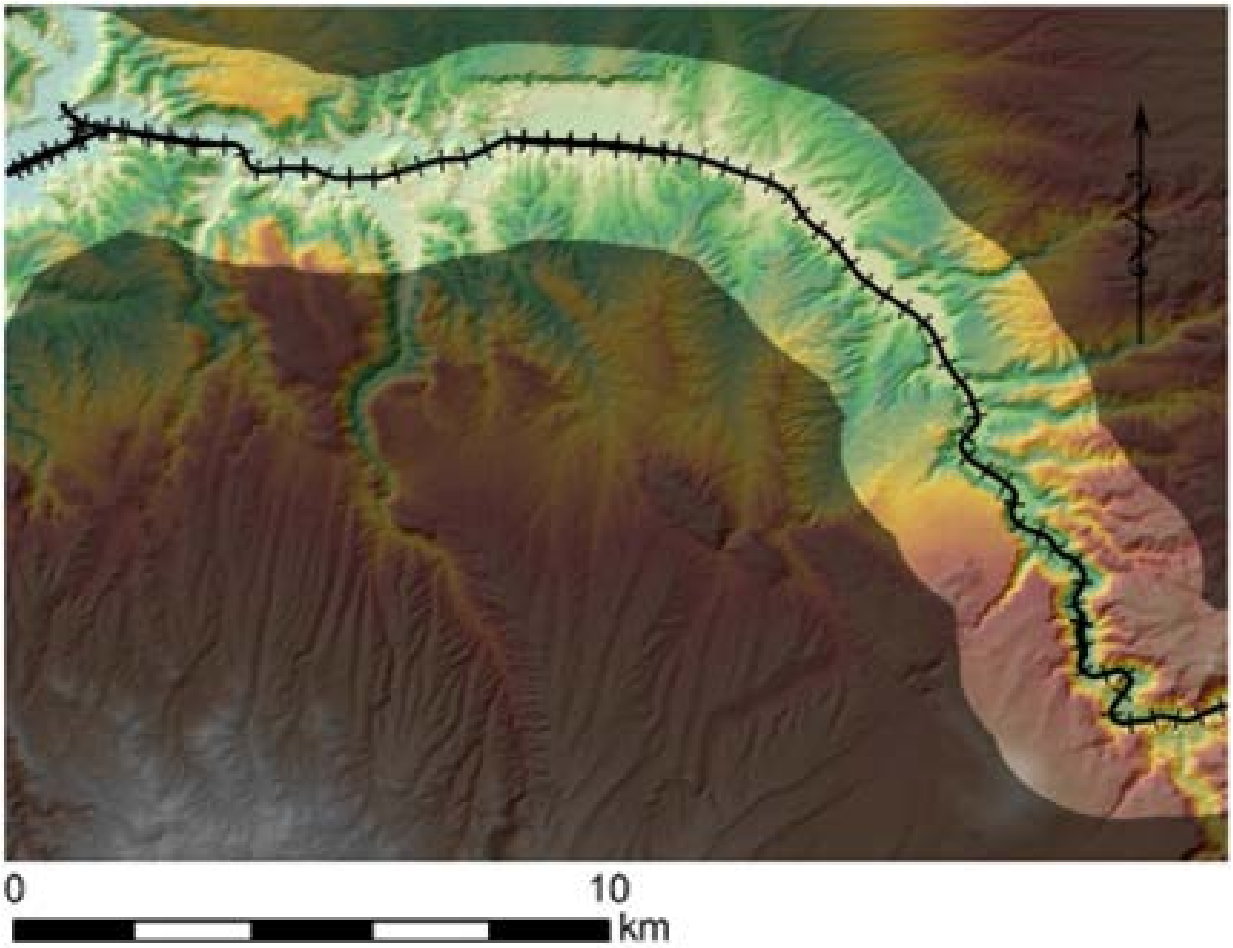

Figure 7. Area within 1 km buffer around the railroad track at the Nevada study case location.

Using a 10 meter DEM from the National Elevation Dataset (NED) that covers all of the United States, we find critical slopes that are more likely to become unstable and be the sources of landslides. To do this we define a 30º threshold slope value, as discussed previously in this report. The slope values are derived from the 10 m DEM, and all pixels with a slope > 30º and within the 1 km buffer are flagged as potentially unstable (figure 8).

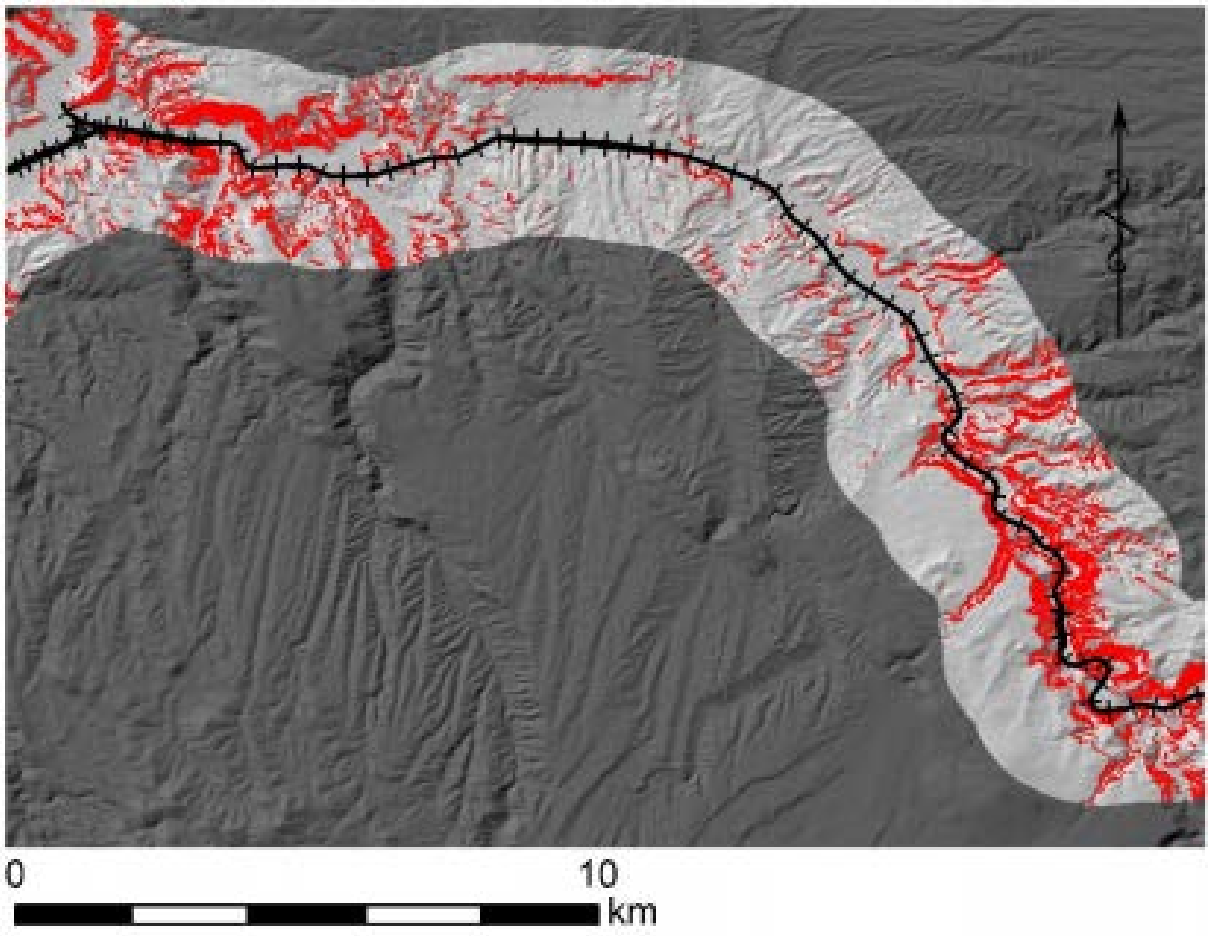

Figure 8. Critical slopes (> 30º) within the 1 km buffer for the study area.

Once potential source areas have been defined, estimating landslide runout becomes the next step, we use the H/L estimation, as explained previously in this report. To be somewhat conservative we use an H/L estimate of 0.25, which on global H/L catalogs (Hunter and Fell, 2002) correlates to the landslide of a large volume (10^5 to 10^6 m^3), although the correlation confidence interval around those values is fairly large (see figure 6 in Hunter and Fell, 2002). Mapping the H/L values to the DEM pixels using the cone approach, and counting the number of times any given pixel falls within a cone with a slope ratio of 0.25 we obtain the map shown in figure 9. Some pixels are in areas that could potentially be exposed to landslides from many different sources, up to 6677 sources in some cases.

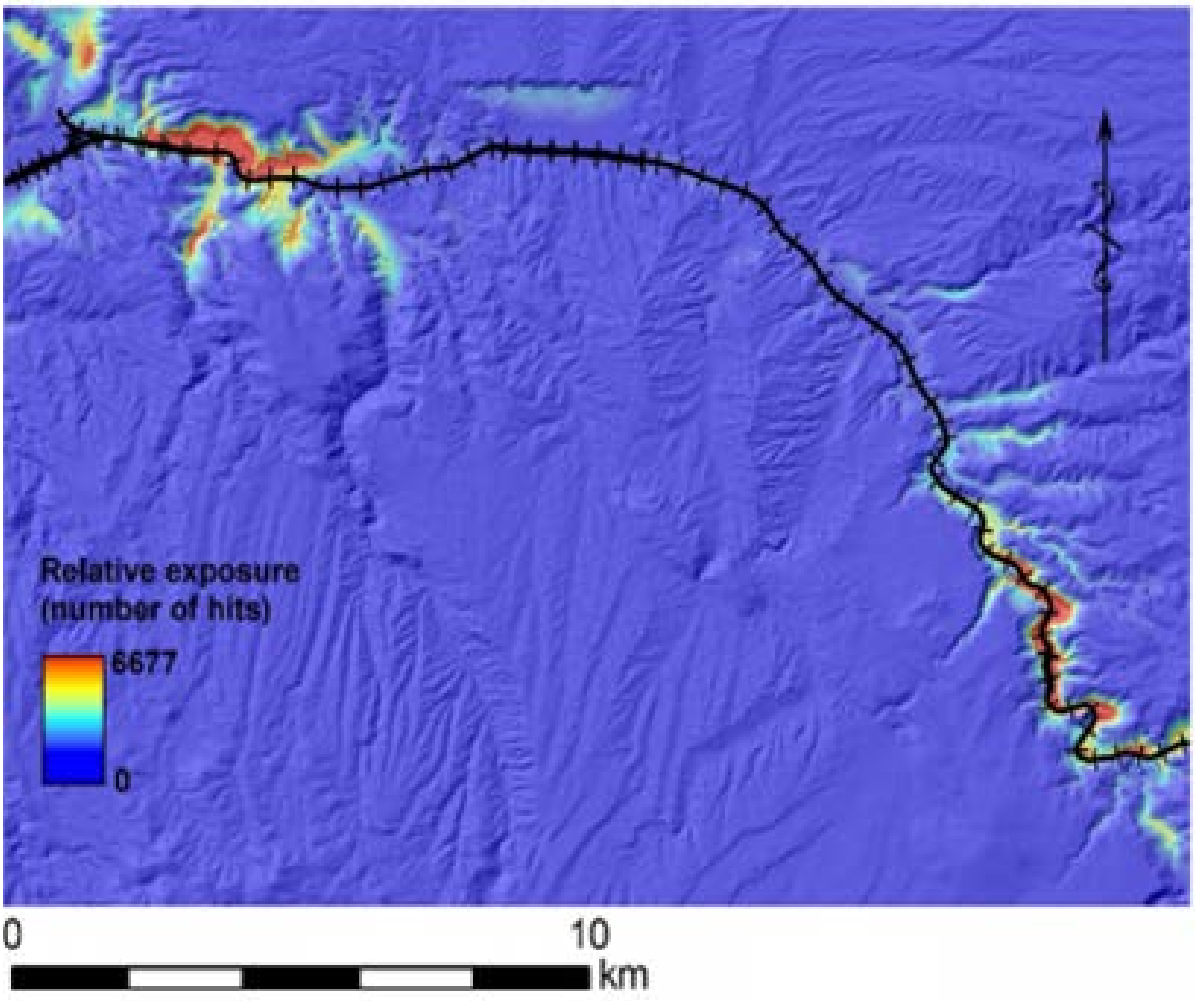

Figure 9. Relative exposure to landslides based on slope and H/L criteria for the study area.

To put this in a relative hazard perspective we show the pixels above the 95 and 99 percentile in the distribution of values given by the number of times a pixel is counted within an exposure cone (figure 10); those areas are the areas with the highest relative exposure according to our method.

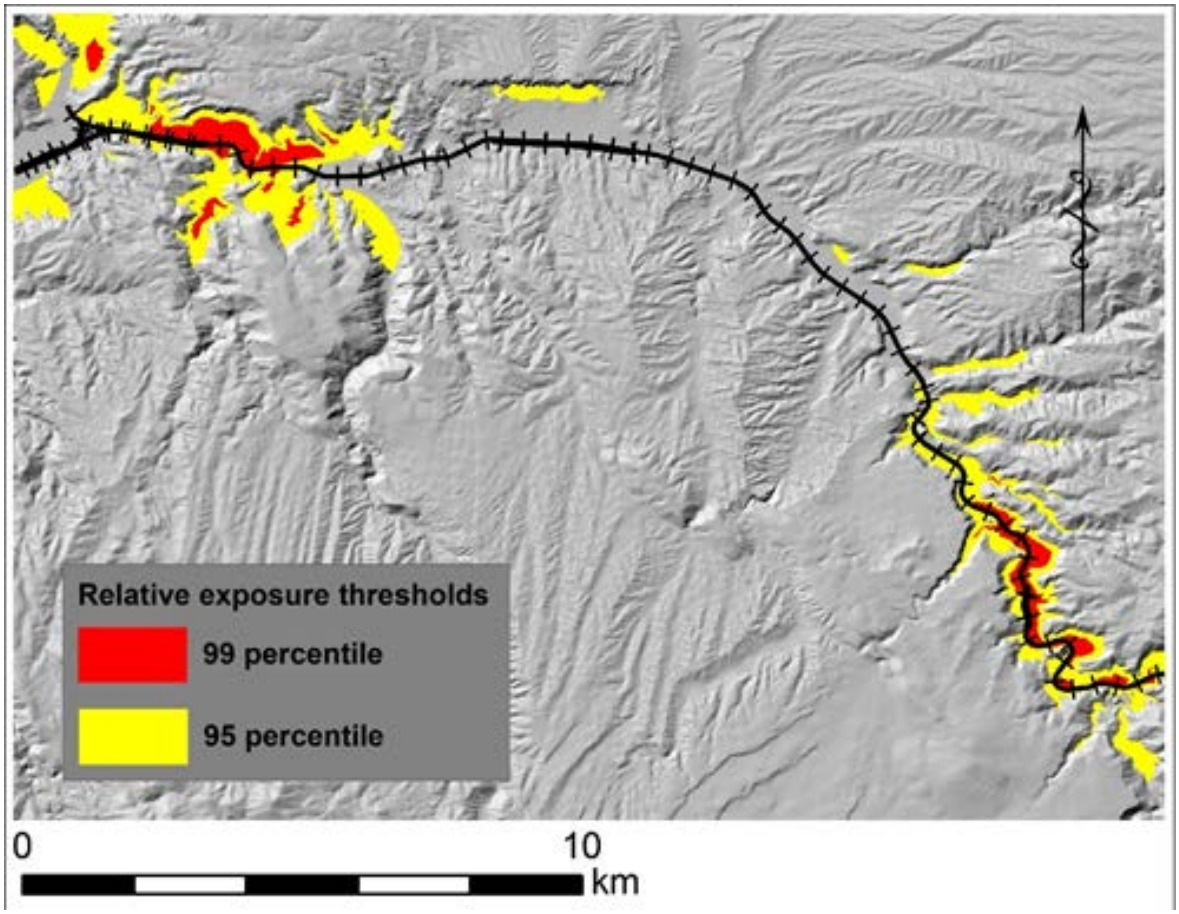

Figure 10. High exposure areas based on the 95 and 99 percentile criteria for the slope and H/L method, in the study area.

Although a large portion of the corridor is outside these high exposure areas, some sections are inside, and those are the sections that may need a more in depth analysis, i. e. they will be considered in the next level of the multi-tier analysis process.

Ground deformation rates can be used to identify hazard areas within the transportation corridor. InSAR stacking techniques, such as PSI, are capable of measuring ground deformation rates down to 1 mm/year. Figure 11 shows InSAR-derived displacement rate (velocity) results from 40 ENVISAT radar images acquired between 2003 and 2010. Areas along the railroad corridor with high displacement rates can be flagged as potentially hazardous. In this case, ground deformation appears to be partially controlled by regional geology and fault lines (Figure 11).

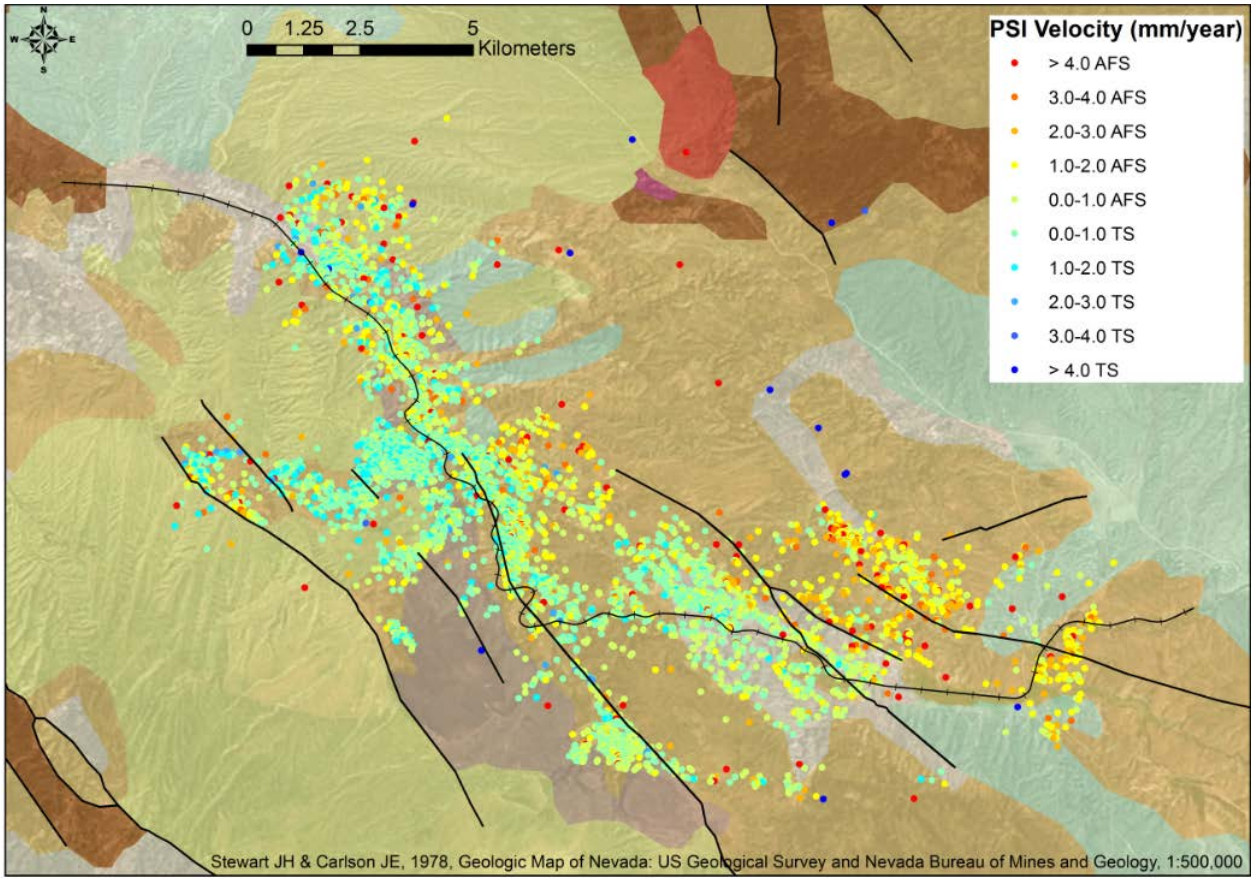

Figure 11: Regional scale InSAR displacement rates (mm/year) along railroad corridor (black dashed line) derived from the PSI stacking technique. PSI velocity shown in LOS direction away from the satellite (AFS) and towards the satellite (TS). Regional geology and faults (black lines) from Stewart & Carlson (1978).

4.1.2. Intermediate and detailed scale analysis

Traditional intermediate-detailed scale analyses, at the slope-by-slope level, are typically performed in the field. These methods use either in-situ instrumentation (e.g., inclinometers and piezometers) and/or detailed observations to obtain information that will allow for further analyses in the office. An example analysis based on detailed observations is the Rockfall Hazard Rating System (RHRS), developed by Pierson (1991 & 1992) to assign relative hazard scores to slopes within a transportation network in order to rank slopes by potential hazard, which in turn leads to assistance with slope mitigation strategies (e.g., which slopes need the attention first?). The RHRS requires the user to note the following slope characteristics: slope height, ditch effectiveness, average vehicle risk, decision sight distance, roadway width, geologic characteristics (structural condition and rock friction or difference in erosion rates), block

size/volume, climate/presence of water on the slope, and rockfall history. Some of these characteristics are difficult to quantify, especially with limited number of trips to the study site (e.g., rockfall history). There are remote sensing techniques (optical photogrammetry, LiDAR, and InSAR) that are capable of measuring small deformation rates across slopes and can give detailed insights into the displacement history of a slope.

The next level of analysis includes both slope surface geometry and movement analysis, from different sources of remote sensing data. In the case of deformation, InSAR data are used over the entire corridor and sections of interest, like those identified in slope angle and the H/L analysis are studied in further detail.

Analysis of InSAR displacement time-series and Λ-t plots can be applied toward slope monitoring and failure prediction. In the example of this slope on the southeastern Nevada railroad corridor, the slope in question has experienced two forms of slope instability since January 2005: occasional rockfalls and approximately complex rotational (2-5 feet) and extensional (up to 20 feet) displacement. Figure 12 shows the interferometric stacking results from the SqueeSAR™ technique on the study slope (Bouali et al. 2016). A collection of 90 ERS-1, ERS-2, and ENVISAT radar images acquired between 1992 and 2010 were processed. Downslope displacement rates (away from the satellite - AFS) up to 4 mm/year were measured along the unstable slope block, while adjacent slopes displayed rates less than 2 mm/year. The displacement time-series of the three orange points measuring the greatest downslope velocity on the slope face (Figure 12) is shown in Figure 13. The time-series shows that the slope was relatively stable from 1992 to 2005. Then, from 2005 to 2010, there was an increase in slope displacement rates with velocities reaching up to 4 mm/year.

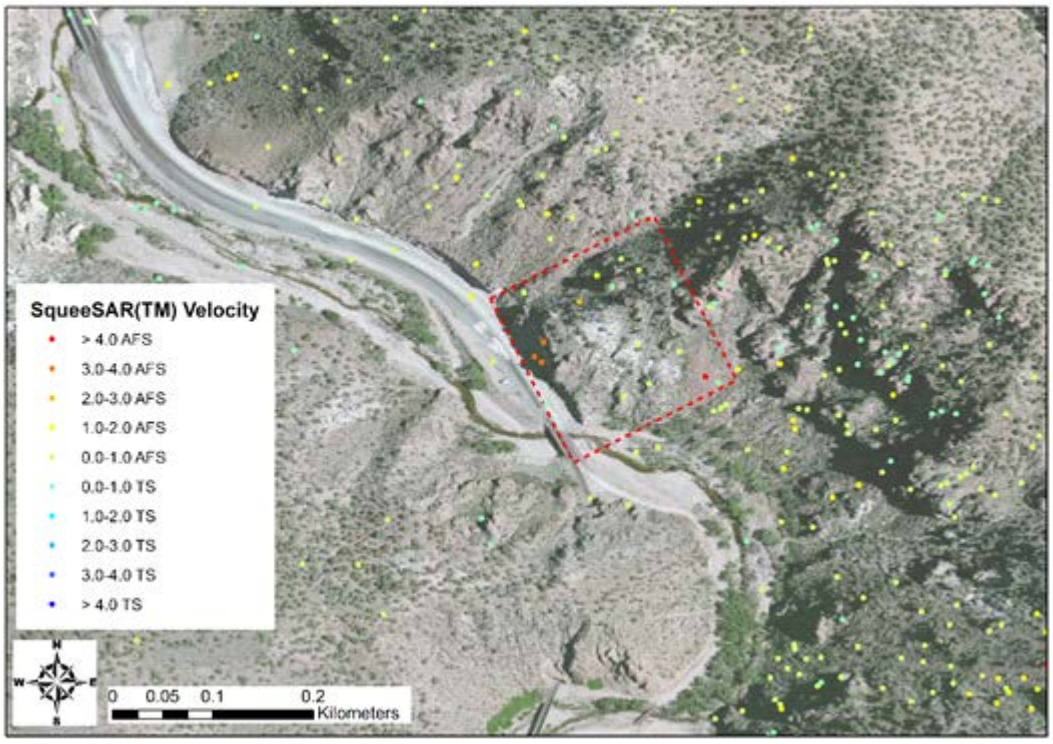

Figure 12: Ground deformation rate (mm/year) measured away from the satellite (AFS) and towards the satellite (TS) across the study area. The slope of interest is located in the red dashed polygon. Image used with permission from Bouali et al. (2016).

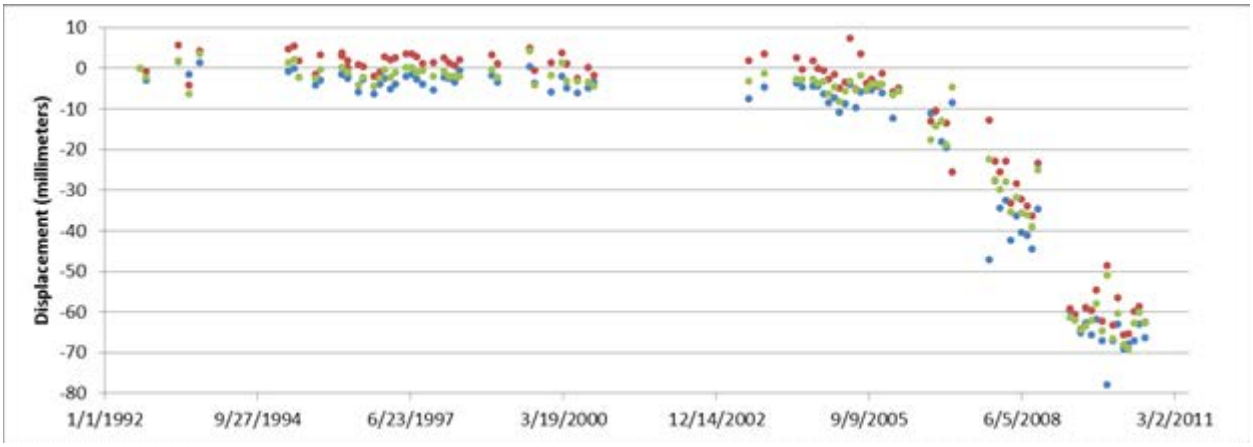

Figure 13: Displacement time-series for three points on slope face (orange points in Figure 12). A negative displacement indicates movement in the downslopes direction (away from the satellite - AFS). Image used with permission from Bouali et al. (2016).

Although the slope has yet to fail, a Λ-t plot was generated for one of the three points from Figures 12 and 13 (Figure 14). The Λ-t plot illustrates the variable amounts of deformation and displacement mechanism

types exhibited within the slope between 1992 and 2010. The slope appears to become more stable (increase in Λ) from 1992 to 2001, where Λ increases from 100 days/mm to almost 1,000 days/mm. Figure 14 (B) shows the Λ-t plot from 2002 to 2010, where the overall Λ-t trend is nonlinear (ductile). Figure 14 (C) then shows the portion of the Λ-t plot (2009-2010) where the overall Λ-t trend has changed to a linear (brittle) inverse velocity curve. This may indicate a change in displacement regime, e.g. a transition from extension displacement to rotational sliding.

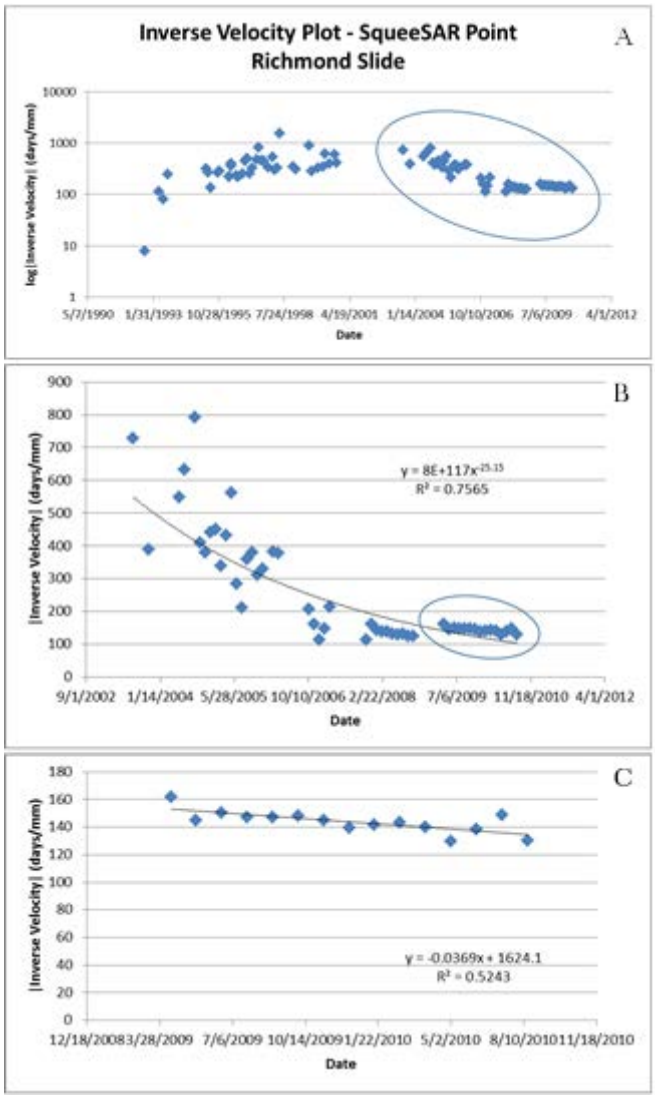

Figure 14: Inverse velocity (Λ) of one point generated from the SqueeSAR™ technique. (A) The full Λ-t plot (1992-2010); (B) partially zoomed-in Λ-t plot (2002-2010, blue oval from (A)); (C) partially zoomed-in Λ-t plot (2009-2010, blue oval from (B)).

Repeated LiDAR dataset from 2011 through 2014 were collected by one of the project partners for one of the critical slopes along the corridor. These datasets were used to analyze the slope movement over time. The displacement analysis (figure 15) shows the movement of large rock blocks, which fell down the slope, leaving large gaps in the slope surface (point clusters shown in blue in figure 15). Deposition of material at the landslide toe also is evident (red areas at the toe of the slope in figure 15).

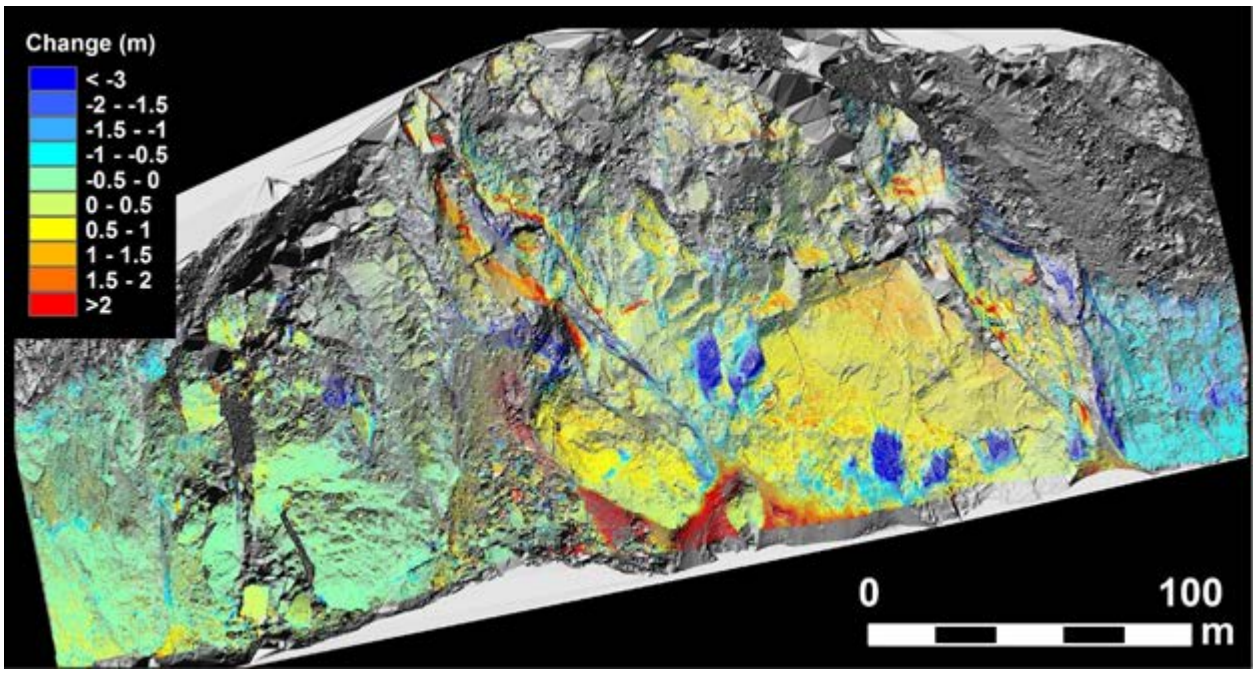

Figure 15. LiDAR derived surface changes at a test slope in Nevada.

More importantly from the hazard perspective, there seems to be a consistent outward movement of a large section of the slope, up to 1 m, shown in yellow colors in figure 15. Such a large movement of the slope could be related to a deep-seated failure of the slope, and a potential major failure affecting the railroad corridor.

Photogrammetry derived point-clouds (figure 16) are also used during this level of analysis. Justice (2015) documented the use of this dataset for the slope analysis of the corridor, in her Master's degree research, as part of this project.

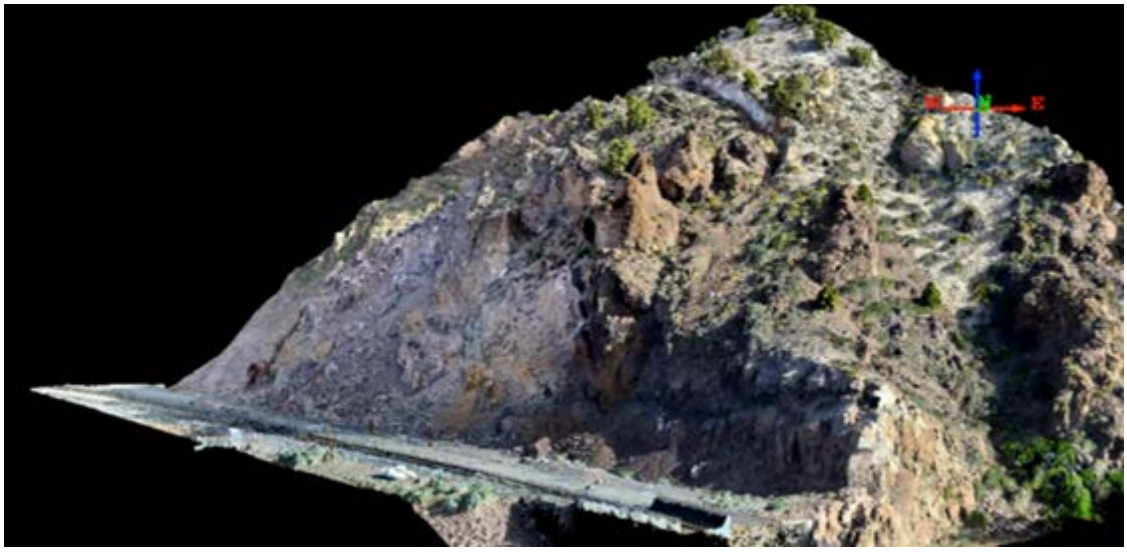

Figure 16. Photogrammetric point-cloud from the test slope in Nevada.

The high resolution and point density of these datasets allows them to be used to measure the orientation and density of discontinuities in the rock-mass. The use of point-clouds for characterizing structural and textural features for rock slopes has been extensively reported in the literature, e. g. Otoo et al. (2013), Jaboyedoff et al. (2007), Martin et al. (2007), Sturzenneger et al. (2009a, 2009b), Dunning et al. (2009), Haneberg (2008), and Dove et al. (2008). Discontinuity orientation mapping using the point-cloud dataset (figure 17), give results that are in good agreement with field mapping orientation for the same rock slope.

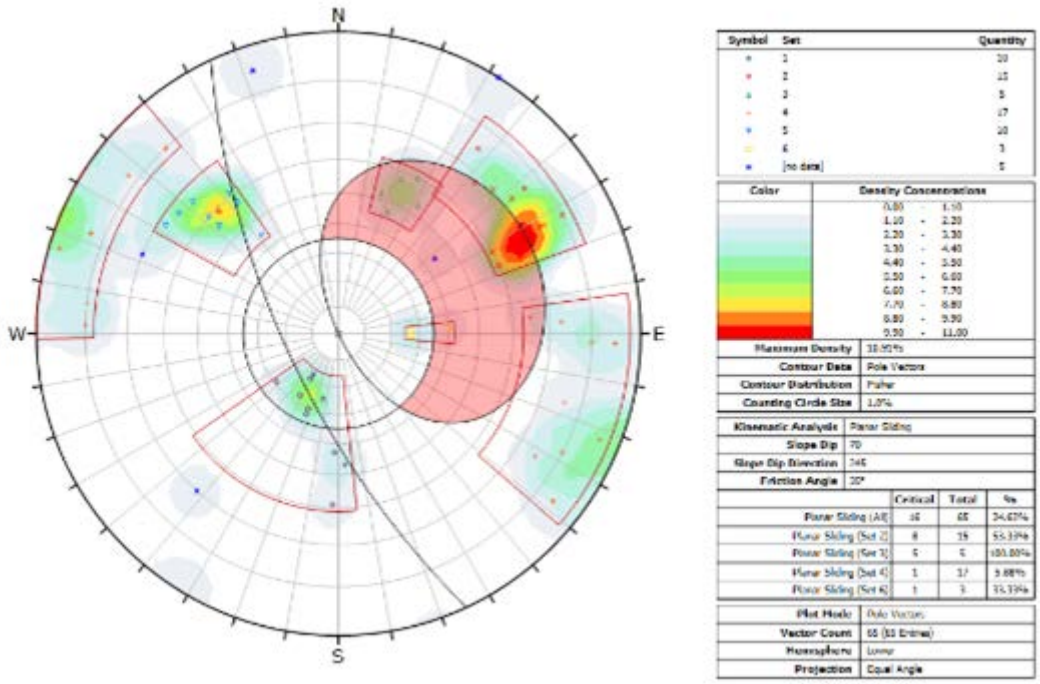

Figure 17. Discontinuities orientation derived from photogrammetric point-clouds from the test slope in Nevada.

The point-cloud is used to generate a high resolution (10 cm pixel) DEM (figure 18), from which profiles are extracted to be used in two-dimensional modeling of the slope stability using computer software.

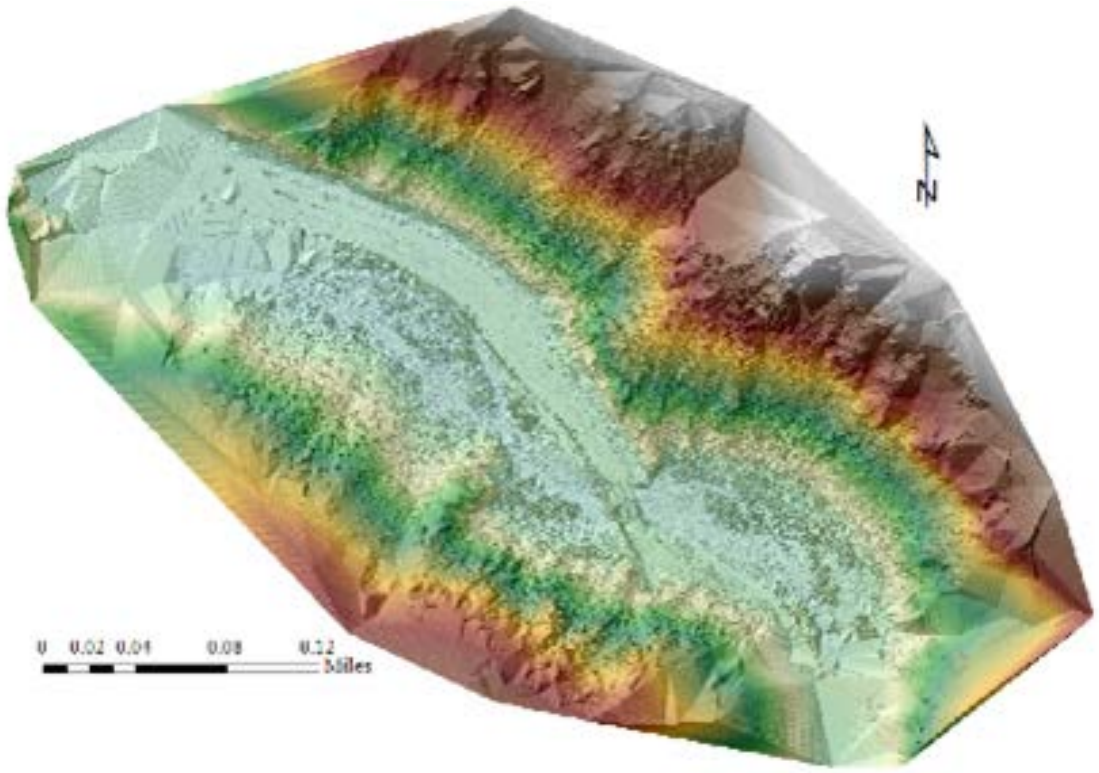

Figure 18. Elevation colored hillshade map, derived from photogrammetric point-clouds from the test slope in Nevada.

The RockScience RocFall and Swedge modules were used to analyze hypothetical scenarios for rockfall and landslide at one of the critical sites. The results show that multiple failure modes are possible for the rock slope, depending on the rock properties and the presence of weak zones within rock mass (figure 19). A more in depth geotechnical analysis is beyond the scope of this report, but our example illustrates how the output of the photogrammetric generated point-cloud can be used as an input, together with other data (e. g. soil or rock-mass properties sampled in the field) to perform such detailed analyses.

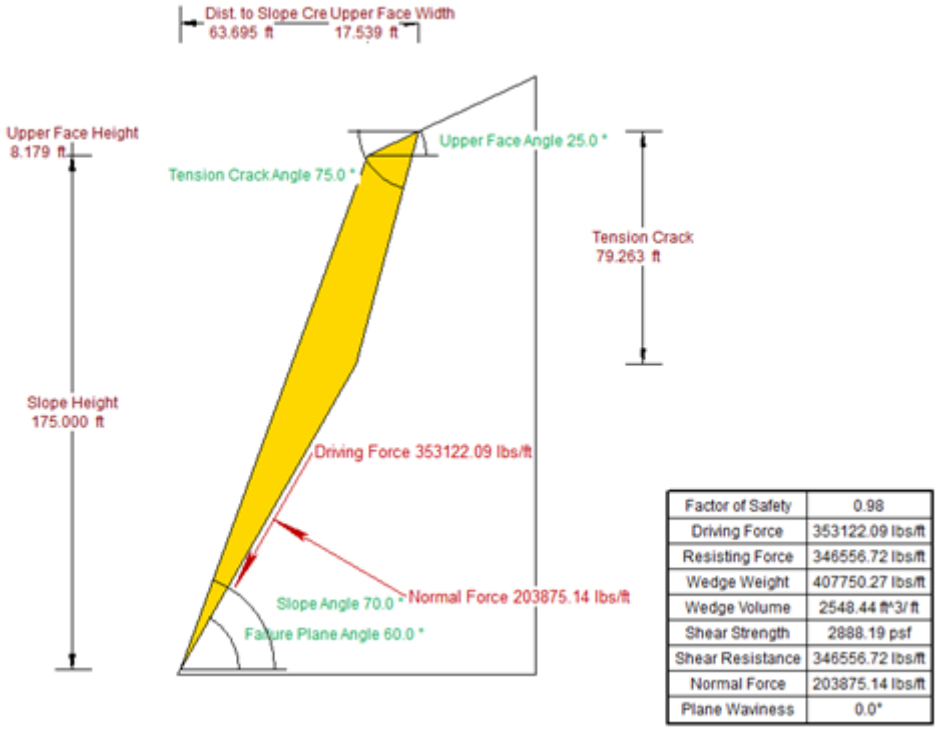

Factor of Safety	0.98
Driving Force	353122.09 lbs/ft
Resisting Force	346556.72 lbs/ft
Wedge Weight	407750.27 lbs/ft
Wedge Volume	2548.44 ft^3/ ft
Shear Strength	2888.19 psf
Shear Resistance	346556.72 lbs/ft
Normal Force	203875.14 lbs/ft
Plane Waviness	0.0°

Figure 19. Example of the slope stability analysis using the input from the high resolution DEM shown in figure 18.

4.2. Retaining wall in Detroit

The second study case chosen for an example is a series of retaining walls along the M-10 highway in Detroit, Michigan. A series of sections of the retaining wall have recently shown significant displacements, causing concern about their stability and the possible damage to the adjacent infrastructure. Retaining wall displacement monitoring was carried out by repeated photogrammetric surveys of the retaining walls. Cerminaro (2014) also documented the technique for his Master's degree research, as part of this project.

4.2.1. Large scale analysis

Coarse resolution radar images, such as the 30-m images acquired by the ERS-1 and ERS-2 satellites between 1992 and 2000, are unable to directly identify individual retaining walls. Two problems arise: the first being coarse resolution images contain many transportation assets and distinguishing between multiple assets located within one pixel is impossible; the second being a geometric issue - retaining walls

are vertical structures and, therefore, do not cover a large spatial extent, making it difficult for a slant-range radar sensor to adequately transmit and receive radar waves on the walls. Instead, a sort of indirect InSAR-derived ground deformation approach can be utilized to understand retaining wall condition. InSAR stacking techniques, such as PSI, allow for the measurement of ground deformation rates on structures nearby the retaining walls of interest. Urban environments allow for a high-density of PS points (Figure 19 - compare this to a rural environment in Figure 12). High-density PS point maps allow for the generation of supplemental analyses - such as differential displacement rate calculations across highways, as shown in Figure 20. These indirect measurements allow for regional scale observations of asset network health.

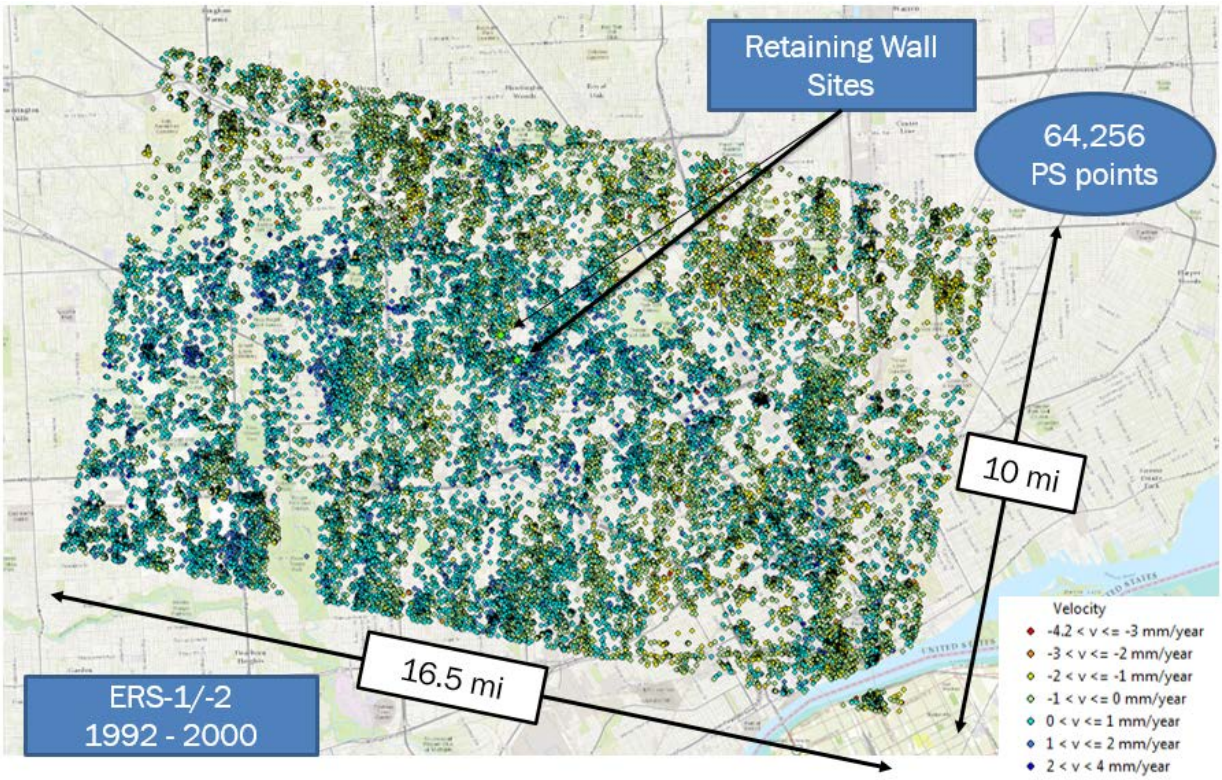

Figure 19: Regional scale PSI displacement rate (velocity) measured within 165 square miles of metropolitan Detroit, Michigan. Negative velocity values indicate displacement rates away from the satellite (subsidence); positive velocity values indicate rates towards the satellite (uplift).

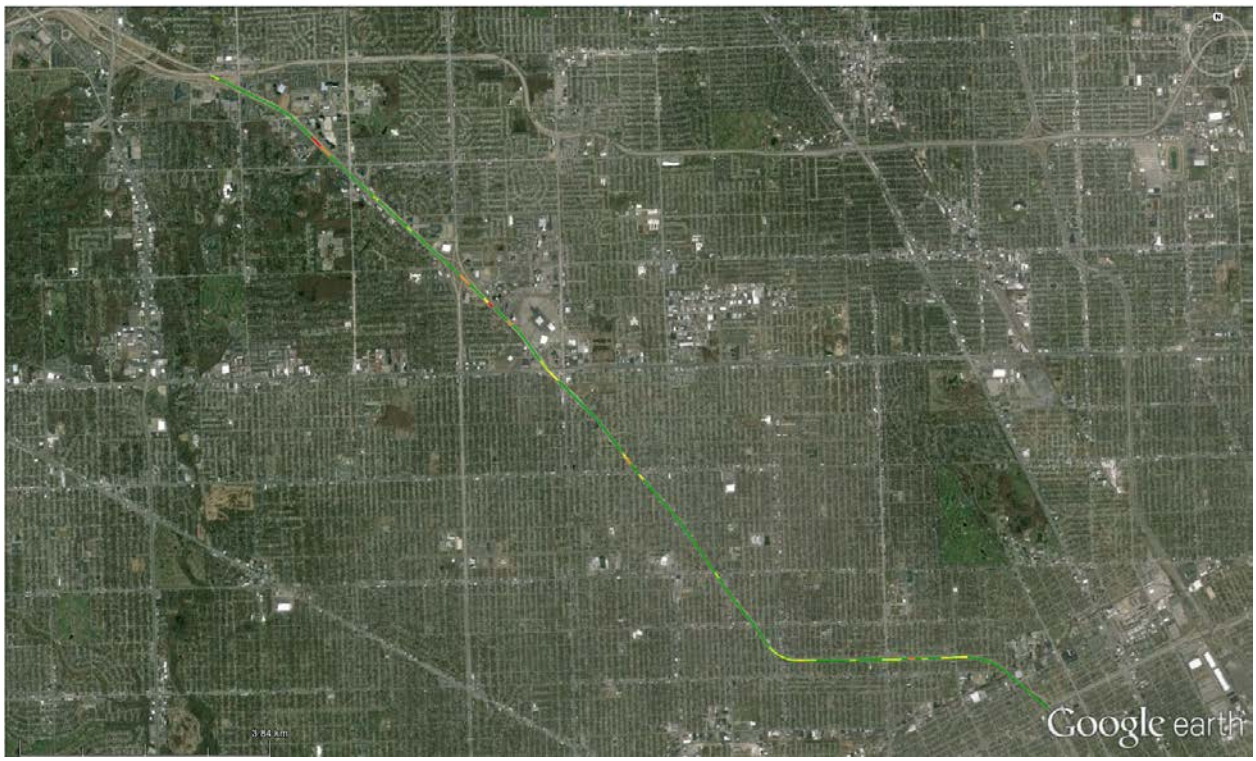

Figure 20: Differential displacement rates (mm/year) measured along a 17-mile stretch of the M-10 Highway, between M-8 and I-696, in metropolitan Detroit. Differential displacement rates measure the variation of displacement rates calculated via PSI-InSAR between 1992 and 2000. The highway is segmented into color zones based on differential displacement rates: green = less than 0.5 mm/year; yellow = 0.5-1.0 mm/year; orange = 1.0-1.5 mm/year; red = 1.5-2.0 mm/year.

4.2.2. Intermediate and detailed scale analysis

The detailed analysis for the retaining walls case is mainly restricted to the deformation measurements of the wall sections. Figure 21 shows some of the problematic retaining wall sections.

Figure 21: Individual retaining wall sections and joints between them, at the M-10 test location

Photogrammetric data were collected across retaining wall sections that where suspected to have moved, at different times in 2014. Point-clouds generated from photogrammetry were used to interpolate rasters parallel to the wall surface, showing the distance perpendicular to the wall face, similar to a DEM but with horizontal distances instead of vertical elevations. Similar rasters were generate for each of the point-clouds collected at different times. Taking the differences between pairs of such rasters, it is possible to see the displacements perpendicular to the retaining wall face between the times at which the images were acquired.

Figure 22 shows a map of the displacements perpendicular to the wall face, through several sections of the wall. Light green colors represent zero or negligible displacement, blue colors represent displacements away from the viewer's perspective and red colors represent movements towards the viewer's perspective. Maximum displacements measured at individual pixels exceed 4 cm in some cases, but such values may be affected by random noise.

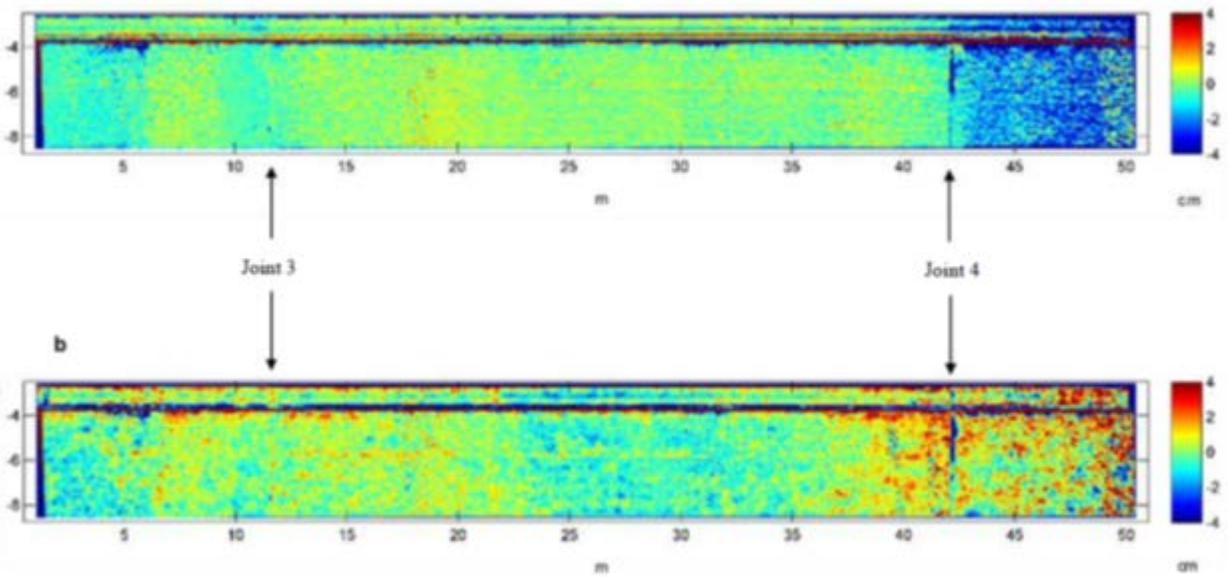

Figure 22: Wall-perpendicular displacement map, for 3 sections of the retaining wall at the M-10 test location.

Analyzing the distribution of measured displacements we observer a distribution of values for all the pixels that resembles a normal distribution (see figure 23). Assuming that the individual wall sections

behave as rigid bodies, the displacement between adjacent sections can be approximated by the mean value of their displacements, or more generally by fitting a plane through the data points for each section.

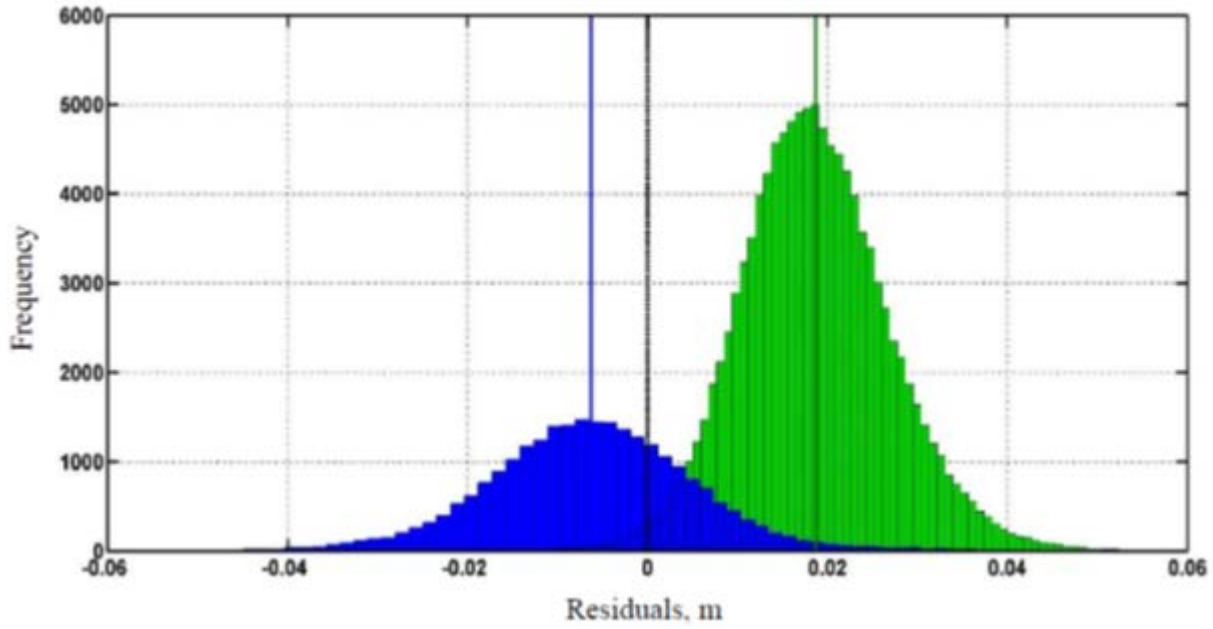

Figure 23: Distribution of wall-perpendicular displacements for the wall sections shown in figures 22 and 23, at the M-10 test location. Some of the dispersion of values may correspond to random noise, but the central values of the distributions are expected to give a highly accurate measurement of the rigid body displacement.

In this way we are able to eliminate the effect of random noise and obtain a more precise measure of the rigid body displacement of the individual wall sections. As figure 23 shows, the displacement of the walls considered in that example amount to 1.9 and 0.6 cm.

A similar analysis can be done for all sections of the wall that are suspected to be moving, and the movement pattern can be used to infer the potential failure mechanism. Figure 24 shows the displacement for two wall joints, and the top-view interpretation of the wall sections movement.

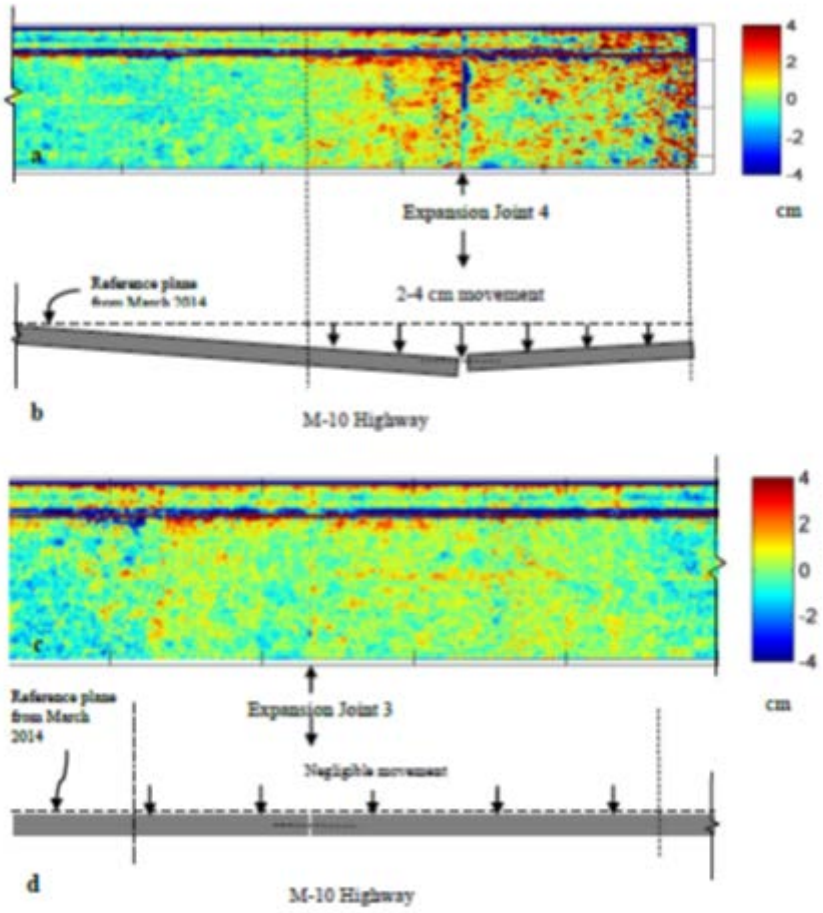

Figure 24: Wall-perpendicular displacement maps and top-view interpretations of the corresponding wall movements, for 2 sections of the retaining wall at the M-10 test location.

The results of the photogrammetric displacement analysis can then be used to infer possible failure mechanisms, and the need to mitigate (or not) the potential wall failure problem. The details of such an analysis will depend on the wall design, the backfill properties and other factors. Such an analysis is beyond the scope of this report, but the use of remote sensing (photogrammetry based in this case) derived displacement values illustrates how our proposed methods can be a valuable input into more detailed geotechnical analysis.

5. Conclusions.

Geotechnical assets are sometimes ignored or not included in the transportation asset management system concept. Several reasons may be responsible for this, including the difficulty to establish long term

expectations on the asset's performance and life-cycle behavior. This is complicated by the requirement of monitoring the health state of geotechnical assets that may require expensive and high resource consuming methods, e. g. geotechnical in situ and laboratory testing, analytical modeling, etc.

Monitoring the surface displacement or deformation of geotechnical assets can be a highly valuable for the geotechnical asset monitoring purpose, as surface deformation can be used in many cases to infer the internal, and in general, the overall state of the asset. Field methods (e. g. precision surveying) to measure displacement or deformation may be as expensive and resource intensive as some of the other geotechnical methods used to monitor the state of the assets. In this project we propose to use remote sensing methods to identify and measure surface displacements at different geotechnical assets. Specific cases of slopes and retaining walls are tested using InSAR, LiDAR and photogrammetric techniques.

Other information also produced by the proposed remote sensing methods include high resolution surface geometry models for the surveyed assets, which can be further used for characterize the state of the assets, e. g. by studying the texture and structural features, like discontinuity orientations in rock slopes, that can also be retrieved from the high resolution three-dimensional point clouds.

The remote sensing data, including the deformation measurements can be incorporated in existing schemes to assess geotechnical assets, like the "Rockfall Hazard Rating System" proposed by Pierson (1992, 1993). At a more general level, we propose a multi-tier approach in which different levels of analysis are followed, starting with a large scale, low resolution level in which the most critical areas are identified and flagged for further in depth analysis, at the following levels of the process. At each level the analysis output gives a diagnostic of the asset as either not needing immediate attention, or in need of further actions. If further actions are needed, they are grouped in two categories: further analysis, if the current level is non-conclusive enough, or a set of explicit actions that have to be taken to avoid the asset deterioration and loss of performance. In this project we do not explore the details of the most detailed level of analysis, which would typically require specific geotechnical analyses that go beyond the scope of this work, but our results show how the output of the remote sensing methods that we use, can be the input for more detailed types of analysis.

6. References

Anderson, Scott A., Daniel Alzamora, and Matthew J. DeMarco. "Asset Management Systems for Retaining Walls." *GEO-Velopment@s The Role of Geological and Geotechnical Engineering in New and Redevelopment Projects*. ASCE, 2008.

Anderson SA & Rivers BS, 2013, Corridor Management: A Means to Elevate Understanding of Geotechnical Impacts on System Performance. *Transportation Research Record: Journal of the Transportation Research Board*, No. 2349, 9-15.

Angeli M-G, Gasparetto P, Pasuto A, & Silvano S, 1989, Examples of landslide instrumentation (Italy). *Proceedings of the 12th International Conference on Soil Mechanics and Foundation Engineering*, Rio de Janeiro, 3, 1531-1534.

ARUP 2010. Risk-based framework for geotechnical asset management: Phase 2 Report. http://www.highways.gov.uk/knowledge/publications/a-risk-based-framework-for-geotechnical-asset-management/ (accessed on December 20th 2015).

Ashmawy, Alaa, Retaining Walls: Analysis and Design. In: Gunaratne, Manjriker, ed. *The foundation engineering handbook*. CRC Press, 2013.

Austroads, 1997, Strategy for improving asset management practices. Austroads Incorporated, Sydney, Australia.

Badger TC, Fish M, & Trople T, 2013, Management of unstable slopes along Washington State highways - past, present, and future. *ASCE Geo-Congress 2013*, 1650-1657.

Bouali EH, Escobar-Wolf R, Oommen T, 2015, Ground Feature Monitoring Using Satellite Imagery: How Interferometric Stacking of SAR Can Mitigate Geo-Disasters along Transportation Corridors. *ASCE Geostrata*, 2015(4), 38-44.

Bouali EH, Oommen T, & Escobar-Wolf R, 2016, Interferometric stacking toward geo-hazard identification and geotechnical asset monitoring. *ASCE Journal of Infrastructure Systems* [accepted].

Brutus, Olivier, and Gil Tauber. *Guide to asset management of earth retaining structures*. US Department of Transportation, Federal Highway Administration, Office of Asset Management, 2009.

Cambridge Systematics, Inc., Parsons Brinckeroff Quade & Douglas, Inc., Roy Jorgensen Associates, Inc., & Thompson PD, 2002, Transportation Asset Management Guide. American Association of State Highway and Transportation, Washington, D.C., 134 pages.

Cerminaro DJ, 2014, Implementation of Photogrammetry to Improve Proactive Assessment of Retaining Walls along Transportation Corridors. *Michigan Technological University MS Thesis*, 69 pages.

Clayton, Chris RI, Rick Woods, Andrew Bond, and Jarbas Milititsky. *Earth pressure and earth-retaining structures*. CRC Press, 2014.

Corominas, Jordi. "The angle of reach as a mobility index for small and large landslides." *Canadian Geotechnical Journal* 33.2 (1996): 260-271.
DeMarco MJ, Barrows RJ, & Lewis S, 2010, NPS Retaining Wall Inventory and Assessment Program (WIP): 3,500 Walls Later. *ASCE Earth Retention Conference 3 (ER2010)*, 870-877.

Dove, Joseph E., et al. "Remote characterization of rock exposures using terrestrial LIDAR." *Proc. of GeoCongress* (2008): 61-61.

Dunning, S. A., C. I. Massey, and N. J. Rosser. "Structural and geomorphological features of landslides in the Bhutan Himalaya derived from terrestrial laser scanning." *Geomorphology* 103.1 (2009): 17-29.

Dzurisin D & Lu Z, 2007, Interferometric Synthetic Aperture Radar (InSAR). In: Volcano Deformation: Geodetic Monitoring Techniques, edited by Dzurisin D, Chichester: Praxis Publishing Ltd., 153-194.

Federal Highway Administration (FHWA), 1999, Asset Management Primer. U.S. Department of Transportation, Washington, D.C., 30 pages.

Federico A, Popescu M, Elia G, Fidelibus C, Internò G, & Murianni A, 2012, Prediction of time to slope failure: a general framework. *Environmental Earth Science*, 66, 245-256.

Ferretti A, Prati C, & Rocca F, 2001, Permanent scatterers in SAR interferometry. *IEEE Transactions on Geoscience and Remote Sensing*, 39(1), 8-20.

Finlay, P. J., G. R. Mostyn, and R. Fell. "Landslide risk assessment: prediction of travel distance." *Canadian Geotechnical Journal* 36.3 (1999): 556-562.

Flintsch GW & Bryant, Jr. JW, 2006, Asset management data collection for supporting decision processes. U.S. Department of Transportation, Washington, D.C., 97 pages.

Fukuzono T, 1985, A new method for predicting the failure time of a slope. *Proceedings from the IV International Conference and Field Workshop on Landslides*, Tokyo, Japan, 145-150.

Glendinning S, Hall J, & Manning L, 2009, Asset-management strategies for infrastructure embankments. *Proceedings of the Institution of Civil Engineers: Engineering Sustainability*, 162(ES2), 111-120.

Haneberg, William C. "Using close range terrestrial digital photogrammetry for 3-D rock slope modeling and discontinuity mapping in the United States."*Bulletin of Engineering Geology and the Environment* 67.4 (2008): 457-469.

Hooper A, Zebker H, Segall P, & Kampes B, 2004, A new method for measuring deformation on volcanoes and other non-urban areas using InSAR persistent scatterers. *Geophysics Research Letters*, 31(23), 1-5.

Hsü, Kenneth J. "Catastrophic debris streams (sturzstroms) generated by rockfalls." *Geological Society of America Bulletin* 86.1 (1975): 129-140.

Huang SL, Darrow MM, & Calvin P, 2009, Unstable Slope Management Program: Background Research and Program Inception - Phase I Final Report (August 2009). *Alaska Department of Transportation and Public Facilities*, 90 pages.

Hungr, Oldrich, Serge Leroueil, and Luciano Picarelli. "The Varnes classification of landslide types, an update." *Landslides* 11.2 (2014): 167-194.

Hunter, Gavan, and Robin Fell. "Travel distance angle for" rapid" landslides in constructed and natural soil slopes." *Canadian Geotechnical Journal* 40.6 (2003): 1123-1141.

Jaboyedoff, Michel, Jean-Paul Dudt, and Vincent Labiouse. "An attempt to refine rockfall hazard zoning based on the kinetic energy, frequency and fragmentation degree." *Natural Hazards and Earth System Science* 5.5 (2005): 621-632.

Jaboyedoff, M., et al. "New insight techniques to analyze rock-slope relief using DEM and 3D-imaging cloud points: COLTOP-3D software." *Rock mechanics: Meeting Society's Challenges and demands*. Vol. 1. 2007.

Jaboyedoff, M., and V. Labiouse. "Technical Note: Preliminary estimation of rockfall runout zones." *Natural Hazards and Earth System Science* 11.3 (2011): 819-828.

Justice SM, 2015, Application of a Hazard Rating System for Rock Slopes along Transportation Corridor using Remote Sensing. *Michigan Technological University MS Thesis*, 90 pages.

Kilburn CRJ & Petley DN, 2003, Forecasting giant, catastrophic slope collapse: lessons from Vajont, Northern Italy. *Geomorphology*, 54, 21-32.

Martin, C. D., D. D. Tannant, and H. Lan. "Comparison of terrestrial-based, high resolution, LiDAR and digital photogrammetry surveys of a rock slope."*Proceedings 1st Canada–US Rock Mechanics Symposium, Vancouver*. 2007.

Michigan Department of Transportation (MDOT), 2015, Asset Management at MDOT. http://www.michigan.gov/mdot/0,4616,7-151-9621_15757-25283--,00.html.

Mikkelsen PE, 1996, Field Instrumentation (Chapter 11). In: Landslide Investigation and Mitigation Special Report 247, edited by Turner AK & Schuster RL, Transportation Research Board, National Academy Press, Washington, D.C., 278-317.

Otoo, James N., et al. "Verification of a 3-D LiDAR viewer for discontinuity orientations." *Rock mechanics and rock engineering* 46.3 (2013): 543-554.

Petley DN, 2004, The evolution of slope failures: mechanisms of rupture propagation. *Natural Hazards and Earth System Sciences*, 4, 147-152.

Petley DN & Petley DJ, 2004, On the initiation of large rockslides: perspectives from a new analysis of the Vajont movement record. In: Large Rock Slope Failures, edited by Evans SG, Balkema, Rotterdam (NATO Science Series), 77-84.

Pierson LA, 1991, The Rockfall Hazard Rating System. *Oregon Department of Transportation*, 15 pages.

Pierson LA, 1992, Rockfall Hazard Rating System. *Transportation Research Record 1343*, 6-13.

Pierson, Lawrence A., and R. Van Vickle. "Rockfall hazard rating system."*Transportation Research Record* (1992): 6-6.

Rose BT, 2005, Tennessee Rockfall Management System. *Virginia Polytechnic Institute and State University PhD Dissertation*, 107 pages.

Sanford Bernhardt KL, Loehr JE, & Huaco D, 2003, Asset Management Framework for Geotechnical Infrastructure. *Journal of Infrastructure Systems*, 9, 107-116.

Sarmap, 2014, SARscape Help. SARscape (version 5.1).

Stanley, David A. "Asset management in a world of dirt: Emergence of an underdeveloped sector of transportation asset management." *TR News* 277 (2011).

Stanley DA & Pierson LA, 2013, Geotechnical Asset Management of Slopes: Condition Indices and Performance Measures. *Special Publications for Geo-Congress 2013: Stability and Performance of Slopes and Embankments III*, San Diego, California, March 3-6, 1658-1667.

Stewart JH & Carlson JE, 1978, Geologic Map of Nevada: US Geological Survey and Nevada Bureau of Mines and Geology, 1:500,000.

Sturzenegger, M., and D. Stead. "Close-range terrestrial digital photogrammetry and terrestrial laser scanning for discontinuity characterization on rock cuts." *Engineering Geology* 106.3 (2009): 163-182.

Sturzenegger, M., and D. Stead. "Quantifying discontinuity orientation and persistence on high mountain rock slopes and large landslides using terrestrial remote sensing techniques." *Natural Hazards and Earth System Science* 9.2 (2009): 267-287.

Varnes, David J. "Slope movement types and processes." *Transportation Research Board Special Report* 176 (1978).

Vessely M, 2013, Geotechnical Asset Management: Implementation Concepts and Strategies. United States Department of Transportation, Central Federal Lands Highway Division, Publication No. FHWA-CFL/TD-13-003, 73 pages.

Vessely M, Widmann B, Walters B, Collins M, Funk N, Ortiz T, & Liapply J, 2015, Wall and Geotechnical Asset Management Implementation at Colorado Department of Transportation. *TRB 94th Annual Meeting Compendium of Papers*, 1-19.

Voight, 1989, A Relation to Describe Rate-Dependent Material Failure. *Science*, New Series, 243, 4888, 200-203.

Wartman J & Malasavage NE, 2013, Predicting Time-to-Failure in Slopes from Precursory Displacements: A Centrifuge Experiment. *Geo-Congress 2013*, 741-749.